Spring 2013

Characterization of an Evolving Serotonin Transporter Computational Model

Laura Marie Geffert

CHARACTERIZATION OF AN EVOLVING SEROTONIN TRANSPORTER COMPUTATIONAL MODEL

A Thesis

Submitted to the Graduate School of Pharmaceutical Sciences

Mylan School of Pharmacy

Duquesne University

In partial fulfillment of the requirements for

the degree of Master of Science

By

Laura M. Geffert

May 2013

CHARACTERIZATION OF AN EVOLVING SEROTONIN TRANSPORTER

COMPUTATIONAL MODEL

By

Laura M. Geffert

Approved November 12, 2012

_____
Christopher K. Surratt, Ph.D.
Professor of Pharmacology
(Committee Chair)

_____
Jeffry D. Madura, Ph.D.
Professor of Chemistry and Biochemistry
(Committee Member)

_____
Jane E. Cavanaugh, Ph.D.
Assistant Professor of Pharmacology
(Committee Member)

_____
James K. Drennen, III, Ph.D.
Associate Dean, Research and Graduate Programs
Graduate School of Pharmaceutical Sciences

_____
J. Douglas Bricker, Ph.D.
Dean, Mylan School of Pharmacy and the
Graduate School of Pharmaceutical Sciences

ABSTRACT

CHARACTERIZATION OF AN EVOLVING SEROTONIN TRANSPORTER COMPUTATIONAL MODEL

By

Laura M. Geffert

May 2013

Thesis supervised by Dr. Christopher K. Surratt

A major obstacle for developing new antidepressants has been limited knowledge of the structure and function of a central target, the serotonin transporter (SERT). Established SERT inhibitors (SSRIs) were docked to an *in silico* SERT model to identify likely binding pocket amino acid residues. When mutated singly, no one of five implicated residues was critical for high affinity in vitro binding of SSRIs or cocaine. The *in silico* SERT model was used in ligand virtual screening (VS) of a small molecule structural library. Selected VS "hit" compounds were procured and tested *in vitro*; encouragingly, two compounds with novel structural scaffolds bound SERT with modest affinity. The combination of computational modeling, site-directed mutagenesis and pharmacologic characterization can accelerate binding site elucidation and the search for novel lead compounds. Such compounds may be tailored for improved serotonin

receptor selectivity and reduced affinity for extraneous targets, providing superior antidepressants with fewer adverse effects.

TABLE OF CONTENTS

Page

ABSTRACT iv

LIST OF FIGURES vii

CHARACTERIZATION OF AN EVOLVING SEROTONIN TRANSPORTER COMPUTATIONAL MODEL 1

1. INTRODUCTION 1

2. METHODS 16

3. MATERIALS AND EQUIPMENT 24

3. RESULTS 40

AIM 1 40

AIM 2 44

AIM 3 51

4. DISCUSSION 61

5. REFERENCES 85

LIST OF FIGURES

Page

Figure 1: 3D Representation of the SERT Protein created using Dr. Manepalli's SERT model 2

Figure 2: Partial sequence alignment of LeuT and hSERT highlighting protein similarities for transmembranes 9 and 10 5

Figure 3: 3D representation of residues predicted to comprise the binding pockets of SERT using Dr. Manepalli's SERT model 13

Figure 4: hSERT HEK 293 membrane concentration optimization via saturation binding of cocaine or clomipramine 43

Figure 5: Screening for inhibitor binding and substrate uptake at hSERT mutants transiently expressed in N2A neuroblastoma cells 46

Figure 6: One-point binding of compounds in LM series to SERT 52

Figure 7: One-point binding of compounds in SM series to SERT 53

Figure 8: Saturation binding and uptake of VS hit compound SM14 at hDAT HEK293 cells. 55

Figure 9: Structures of two VS hit compounds showing affinity for SERT 57

Figure 10: Saturation binding of VS hit compounds SM10 and SM11 at hSERT HEK293 cells 58

Figure 11: One-point binding of compounds in MS series to SERT 60

Figure 12: Structure of 6-nitroquipazine and one analog tested at hSERT 63

Figure 13: Structures of norfluoxetine (SADU 2-191) and three analogs tested at hSERT……..……..65

Figure 14: Structures of two citalopram analogs tested at hSERT 67

Figure 15: Structures of racemic fluoxetine (SADU 3-89) and two analogs tested at hSERT 69

Figure 16: Structure of Proneurogenic compound P7C3 and analogs created by Dr. David Lapinsky 71

Introduction

A. Serotonin and its modulation in the synapse

Serotonin is a signaling molecule in the brain and in the periphery that functions to regulate mood, weight, sleep, digestive and motor functions. The modulation of serotonin underlies the behavioral effects of various psychoactive drugs. Modulation of the neurotransmitter (NT) has been identified as an important target for a wide range of drugs for the treatment of mood, anxiety, and behavioral disorders. It is inactivated by synaptic clearance, mediated by the serotonin transporter (SERT) protein (Figure 1), a member of the monoamine transporter (MAT) family of proteins. The SERT translocates serotonin across the cell plasma membrane via electrogenic transport, driven by the neuronal inward Na^+ gradient. Co-transport of Cl^- is required of all MATs, and the SERT additionally antiports (exports) K^+. Selective serotonin reuptake inhibitors (SSRIs) and tricyclic antidepressants (TCAs) both inhibit the reuptake of serotonin into the presynaptic neuron, while SSRIs bind selectively to SERT. This results in synaptic pooling of the NT, leading to an increase in downstream signal transduction and propagation of the NT's effects. The binding site for serotonin is formed by some of the 12 SERT transmembrane domains. An extracellular gate formed by connections between two amino acids blocks access to the primary substrate (serotonin) binding site when the transporter is in the closed conformation. This conformation will change when both a substrate and sodium ions are bound, which ensures that transport movement of the substrate across the membrane will be coupled with sodium.

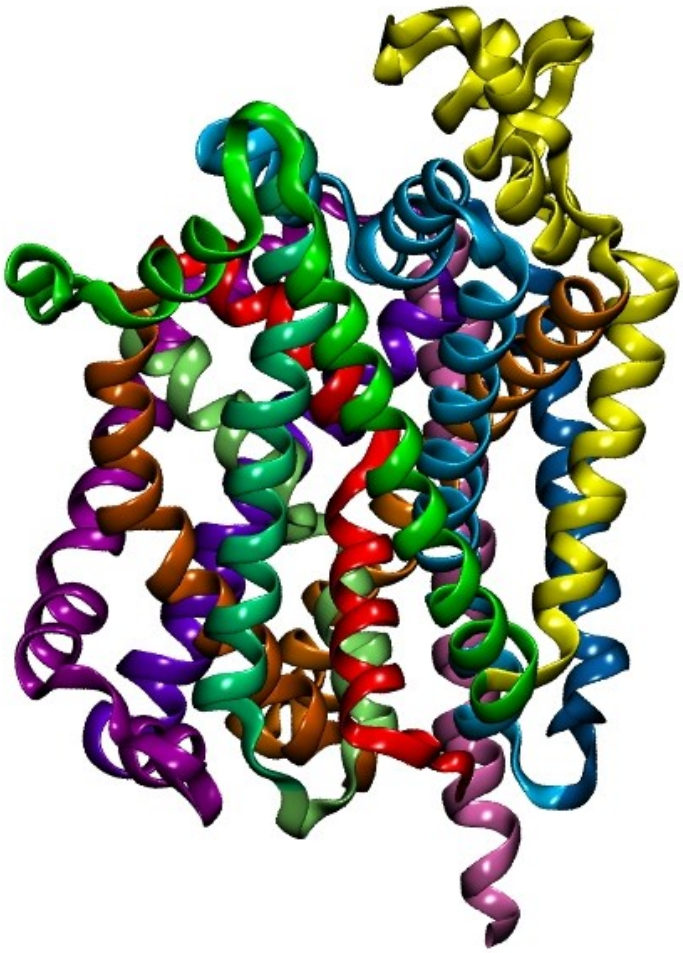

Figure 1: 3D Representation of the SERT Protein using Dr. Manepalli's SERT model. Figure was created using MOE 2008.

B. SERT structure

The sequence of hSERT is comprised of 630 amino acid residues with 12 transmembrane spanning regions (TM domains). Residues conserved among the NSS proteins are typically more important for transporter infrastructure or the translocation mechanism; ones unique to the MATs are more likely to play a role in specificity of substrate binding. Those unique to the SERT may contribute to SSRI binding sites, for example. MAT inhibitor binding site(s) have not yet been reliably defined, and SERT-inhibitor cocrystals do not appear to be pending. Obtaining a MAT X-ray crystal will be difficult, as is the case for most integral membrane proteins. A major challenge of membrane protein crystallography is obtaining and purifying sufficient amounts of the protein. It is challenging to select the proper detergent to ensure the structure of the protein is the same as in the lipid bilayer (Matthew et al., 2006). In the absence of a high-resolution structure, virtual molecular models and biochemical/pharmacological experiments must provide the structure/function information.

C. **Leucine transporter (LeuT) crystallization**

The LeuT bacterial leucine transporter belongs to a family of neurotransmitter/sodium symporters (NSS), also known as the solute carrier 6 (SLC6) gene family. Electrogenic transport of a neurotransmitter substrate across the cell membrane by NSSs is driven by the Na+/K+-ATPase-generated Na+ gradient. Included in this family of symporters are the MATs, distantly-related homologs of LeuT. Prior to the LeuT crystallization, the 3-D structure of NSS proteins was only vaguely understood. Multiple approaches were used to provide clues as to which NSS residues contributed to the general protein

infrastructure, which residues played a role in substrate or ion recognition, and which residues were most likely responsible for a pharmacological pattern unique to a given transporter. MAT primary sequence alignments guided delineation of each TM domain (Goldberg et al., 2003; Surratt et al., 2005). The sequence alignment with SERT (partially shown in Figure 2) also provided clues to NSS structure, which led to many site-directed mutants (Henry et al., 2003). Pharmacological examination of those changes (wildtype protein vs. mutant) can provide notable insights. The substituted cysteine accessibility mutagenesis (SCAM) methodology provides an approach to identify the residues in the membrane-spanning segments that line the transporter and has also contributed to elucidating likely MAT ligand binding cavities and general transmembrane domain infrastructure (Loland et al., 2004; Henry et al., 2006). Unfortunately, these approaches only circumstantially implicate a given residue or protein region as a component of the binding pocket.

The structure of LeuT was crystallized in 2005 (Yamashita et al., 2005). Since LeuT was crystallized, the LeuT crystal has proved to be an excellent template for the construction of experimentally validated models (Beuming et al., 2006; Indarte, et al., 2008). These models have guided numerous site-directed mutagenesis studies for the purpose of characterizing the ligand-protein interactions, which would presumably be correlated with behavioral activity (Forrest, et al., 2007; Zhou, et al., 2009). In the present study, mutations were chosen based on amino acids conserved at the same position in other NSS transporters, namely the dopamine transporter (DAT), the norepinephrine transporter (NET), and LeuT.

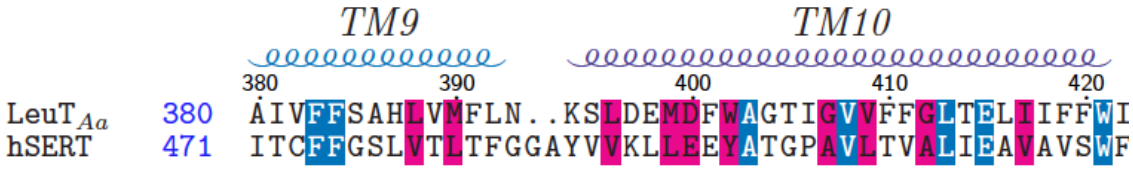

Figure 2: Partial sequence alignment of LeuT and hSERT highlighting protein similarities for transmembranes 9 and 10. Conserved residues are highlighted in blue, residues of similar charges are highlighted in magenta. Figure created and colored by Dr. Tammy Nolan.

Three-dimensional data derived from the LeuT-leucine cocrystal (Yamashita et al., 2005) provided a reliable template for MAT models, even though only 25% amino acid sequence identity and 45% similarity are observed (Beuming et al., 2006). Importantly, LeuT and MATs apparently share the same mechanism of transport. Crystallization of this bacterial MAT homolog has spawned the creation of 3D MAT molecular models that are predicting important residues for inhibitor binding. Such models guide molecular pharmacological studies; a SERT residue predicted from the model to contribute to its functional properties can be mutated and pharmacologically characterized for changes in transport or inhibitor binding properties. In spite of the functional importance of this transporter and its inhibitors, much remains unknown about the structural basis of inhibitor function at binding sites of the serotonin transporter.

D. SERT binding of ligands

It is assumed that a therapeutic with a novel scaffold could reduce affinity for extraneous targets, thereby decreasing unwanted side-effects. In order to rationally create novel medications for disorders associated with SERT, it would be helpful to know how existing therapeutics operate at the molecular level. Transporters must open and close to allow passage of ions and endogenous and/or exogenous ligands. As mentioned above, substrate influx is accomplished by substrate binding when the external gate is open. The internal gate opens when the external gate closes and the substrate can dissociate to the cytoplasmic region. The internal gate can only be open when the external gate is closed,

and vice versa. Multiple residues likely contribute to this conformational change of the protein in a concerted effort involving hydrophilic loops as well as the transmembrane domains. The substitution of some residues may simply interrupt the infrastructure of the protein, but changing residues that play a role in substrate or ion recognition is likely to disrupt binding patterns and therefore disrupt the pharmacological profile of known inhibitors (Barker et al, 1998). Based on previous characterization of the SERT and other NSS proteins, some transmembrane domains have been implicated as important participants in the formation of binding pockets. TMs 1 – 10 of LeuT form the essential core. This core would be a logical place to expect to find a substrate or inhibitor binding pocket or pockets. The TM1 and TM6 domains have the highest density of conserved MAT residues. TM11 and TM12 were found to be outside of the substrate/ion pore created with TMs 1-5 and TMs 6-10 (Yamashita et al., 2005). A serine residue present in TM7 of the MATs serves as the Cl^- cofactor that stabilizes Na^+ binding and thereby leads to the subsequent translocation of the substrate (Forrest et al., 2007). In the LeuT crystal, its substrate (leucine) was found midway through the lipid bilayer in a pocket created by the unwound portions of TM1 and TM6. Coincidentally, these unwound portions of TM1 and TM6 are also thought to act as pivots for the transporter's conversion between the outward- and inward-facing conformations.

In addition to the primary ligand binding pocket at the TM1 – TM6 midpoint, a secondary pocket in the MAT extracellular vestibule region has been implicated in substrate/inhibitor binding. Unwinding of TM1 and TM6 exposes main chain carbonyl oxygen and nitrogen atoms that form a hydrogen bond to the substrate and the sodium

ions. The external gate is composed of one arm between TM1 and TM10 and another arm between TM3 and TM8, and binding of the substrate may be governed by the opening and closing of the gates, thereby regulating the binding of inhibitors. The binding pockets for substrates and inhibitors may overlap (Andersen et al., 2009), or may be completely separate. Tricyclic antidepressant (TCA) drugs have been shown to bind several angstroms above the primary substrate pocket in LeuT crystals. LeuT-TCA cocrystals show a salt bridge formed by TM1 and TM10 (external gate strut) with a water molecule being displaced (Sinning et al., 2009). TCAs have been thought to bind farther into the vestibule of SERT, causing a rotation of the inhibitor that disrupts the salt bridge between Arg104 (TM1) and Glu493 (TM10), opening the "aromatic lid" that covers the pore into the protein. This would allow the ring system of TCAs to be situated between the two gates at the binding site. TCAs and SSRIs were found to bind to distinct regions of the vestibule and prevent substrate uptake by stabilizing the inward conformation (Zhou et al., 2009).

A structural analog is a compound with a structure that is similar to that of another compound, but differing from it in a certain component. It can differ in one or more atoms, functional groups, or substructures, and replaced with other atoms, functional groups, or substructure. A compound can be structurally related to the parent compound, but this similarity does not guarantee functional similarity. Analogs can have different physical, chemical, biochemical, or pharmacological properties than the parent compound. An analog could differ in selectivity for the protein or in ability to inhibit serotonin uptake as compared to the parent compound. They could also be created to

include a cross-linker or a photosensitive group to be used in additional experiments for characterizing the binding pockets. Analogs of known SERT inhibitors can be used and tested for SERT binding and to additionally characterize the binding pockets of the protein. In drug development, structural analogs of an initial lead compound can be tested as part of a structure-activity relationship study. Lack of knowledge about the specific ligand-SERT interactions that lead to their clinical efficacy represents a problem for rationally developing novel therapeutics for SERT-associated disorders.

E. Computational modeling

The elucidation of the SERT 3D structure in the absence of X-ray crystal or NMR data can be addressed using comparative molecular modeling. Comparative, or homology, modeling is based on the proposal that tertiary protein structures are more often conserved than amino acid sequences (Petrey and Honig, 2005). Evolutionarily-related proteins can share comparable physicochemical properties and possess common structural and spatial similarities even if they diverge in their amino acid sequences. Protein structures are more conserved than protein amino acid sequences; therefore, the accuracy and usefulness of the models that can be obtained are positively correlated to the sequence similarity between the template and the target proteins (Pieper et al., 2002). Comparative modeling has been shown to be uncomplicated and typically accurate for proteins that share greater than 40% amino acid sequence identity (Hillisch et al., 2004; Petrey and Honig, 2005). Proteins with less than 30% residue similarity increase the

complexity in creating a homology model, but such models have been successfully generated. These models have guided the creation of other useful models, as well as helped in the virtual screening and pharmacological characterization of other proteins within the same superfamily (Surratt and Adams, 2005).

The technique of homology modeling is used to generate atomic resolution 3D structures of proteins with unknown 3D structures (target), based primarily on alignment with one or more proteins of known 3D structure (templates) evolutionarily related to the target (Petrey and Honig, 2005). In the absence of an experimentally determined structure, a comparative model can provide not only a starting point for experimentally validated research as was done in this study, but also an evolving representation of the target and other structurally-functionally related targets. The four main steps in the process of creating a protein model are template selection, target-template alignment, model building, and model evaluation (Hillisch et al., 2004; Dunbrack, 2006). For the SERT homology model used in this study, LeuT was chosen as the template based on the sequence similarities, which are partially shown in Figure 2. Generation of a reliable computational model is critical for the accuracy of the predictions to be made from the model.

F. Virtual screening

As verified via X-ray structures, similar ligands can bind in different conformations to the same class of protein (Davis et al., 2003). A single protein structure is only useful to identify ligands for that particular conformational state (Carlson and McCammon, 2000). This can prove a challenge when virtually screening a homology model for new potential therapeutics. These proteins often offer multiple binding modes as they shift to allow for the binding of a diverse array of substrates and inhibitors. This potential for diverse compounds to bind to the SERT provides the opportunity to find novel inhibitors.

Docking is a computational technique that assists in predicting the binding modes of ligands within the target protein pocket. The orientation of a ligand within the binding pocket can be predicted by docking (Moustakas et al., 2006). Starting with a large pool of molecules, this digital database is used to evaluate the ability of unknown compounds to dock to the target protein. This digital technique is an alternative to the time-consuming and expensive technique of experimental high throughput screening (HTS). An advantage of this virtual screen is that one may use it to search only for drug-like candidates (Hristozov et al., 2007) and the goal is to find novel-scaffold "hit" compounds in silico with relevant biological and pharmacological activities. As mentioned previously, a novel scaffold could reduce affinity for extraneous targets, something that has plagued SSRIs on the market.

Virtual screening and docking validation attempts to predict how a ligand may bind in the target protein. Experimental pharmacology is necessary to probe how the compounds with high virtual binding scores bind to the target protein. Once hit compounds are chosen, the purchase, based on price and availability, can be carried out and the pharmacological effects of the compounds can be tested experimentally (Evers et al., 2005). The model can then be used as a guide for the position and/or structure of involved functional groups that may interact with an inhibitor (Figure 3). This method of verification can not only assist in the refinement of the model (in a trial-and-error approach of moving amino acid side chains or functional groups), but also in the identification of the SERT binding pocket(s). Unfortunately, the actual percentage of compounds that emerge as hits from virtual screening are typically less than 1% (Bailey and Brown, 2001; Schneider and Bohm, 2002). Also, when X-ray structures are not known and homology models of the target protein are used for the virtual screening process, typically low micromolar (1-10 uM) activities of compounds are found (Anand et al., 2003). Hit compounds of higher affinity to the target protein are more likely to be found when the template and the target share high sequence similarity.

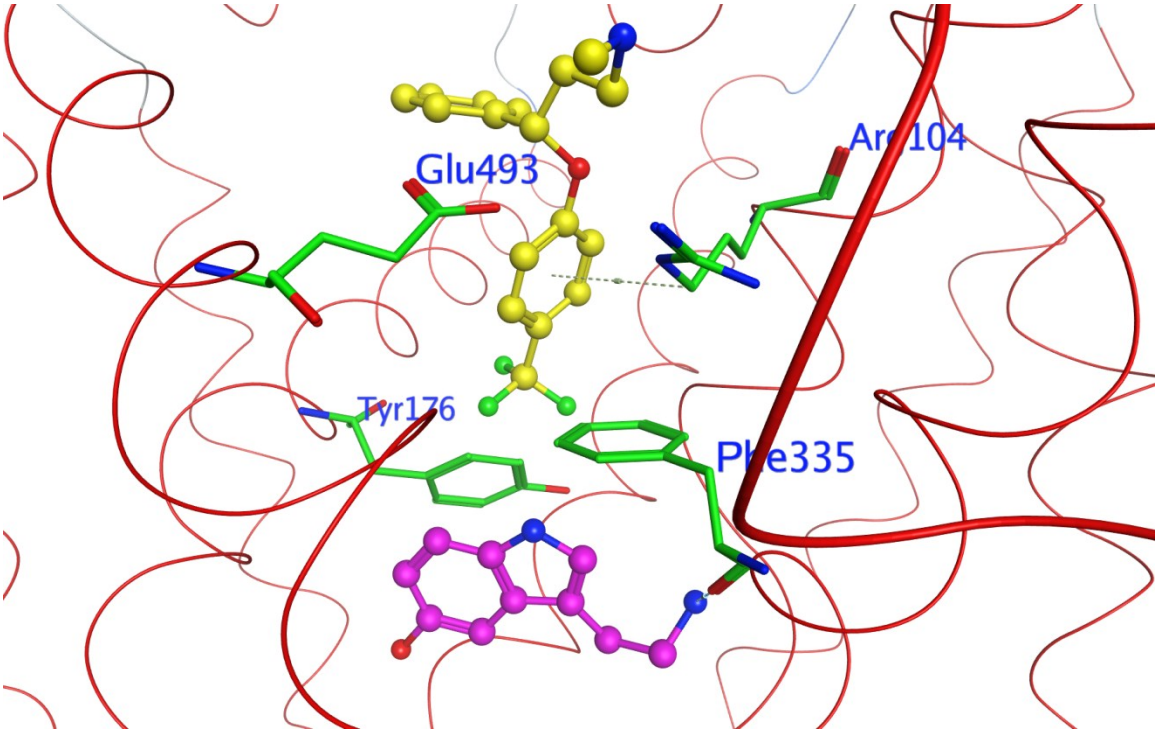

Figure 3: 3D representation of residues predicted to comprise the binding pockets of SERT using Dr. Manepalli's SERT model. Sertraline is colored as yellow within the vestibular pocket and serotonin is colored as magenta in the interior pocket.

G. Clinical Significance

Major Depressive Disorder affects greater than 121 million people world-wide. The economic cost of this disorder, through lost productivity and increased medical expenses, exceeds $83 billion each year. Antidepressants represent the third-largest pharmaceutical category in the world. Depression and its treatment are a large burden on the health care industry, as is the treatment of anxiety. TCAs were the first generation of depression medications. These include drugs with a tricyclic ring structure similar to clomipramine. These compounds resulted in severe side effects due to the lack of selectivity.

Selective serotonin reuptake inhibitors (SSRIs) have more structural variations and are currently considered first for the amelioration of depression, and used for many other mood disorders including anxiety, obsessive-compulsive disorder, and post-traumatic stress disorder. SSRIs selectively bind to the serotonin transporter (SERT), which is well-established as a therapeutic drug target for depression and anxiety. The ability of SSRIs to inhibit neuronal serotonin reuptake, and ultimately lead to an increase in serotonin receptor activation, leads to their effectiveness. Although SSRIs are successful in treating multiple disorders, these drugs have disadvantages such as slow onset of action, sleep disruption, weight gain, and nausea (Moret et al, 2009). During the first few weeks of SSRI use, more serotonin is available, but a downregulation of 5-HT2A postsynaptic receptors occurs, which decreases the possible activation of the postsynaptic neuron (Eison and Mullins, 1996). The additional serotonin also activates presynaptic autoreceptors, which serve as feedback sensors for the cell. Activation of the

autoreceptors will trigger a decrease in serotonin production and therefore a decrease in serotonin release. These neurophysiological adaptations to SSRI use make necessary multiple weeks of treatment prior to the behavioral benefits. Also, the ligand-protein interactions that lead to the clinical efficacy of SSRIs remain unknown. The SSRIs most often prescribed are compounds of diverse structure. Understanding the molecular actions of therapeutics at SERT would aid in the rational design of novel treatments for these mood disorders.

The hypothesis of the presented study is: A computer-generated SERT model can guide structure-function studies on the protein and screen *in silico* small molecule libraries toward discovery of lead compound therapeutics of novel scaffold.

The varied methods mentioned in this brief introduction, including the use of an in silico SERT model, mutagenesis, and virtual screening, can be used in conjunction with one another in order to determine the structure of SERT and find therapeutic inhibitors with novel structural scaffolds. Structurally novel SERT inhibitors can be rationally designed to bind with higher affinity or selectivity for SERT over other MATs. Achieving selectivity for SERT would minimize the side effects seen in the older generation of antidepressants (tricyclic antidepressants) as well as in SSRIs. Therefore, there is an urgent need for novel hSERT inhibitors with improved clinical characteristics. A major goal of this research is to elucidate the structure of SERT and use this information to find or design new therapeutics for the treatment of serotonin-related disorders.

Methods

CELL CULTURE

A stably-transfected WT hSERT HEK cell line employed in the study was grown in DMEM media (with 10% fetal bovine serum, 10% penicillin/streptomycin, and 20 mM L-glutamine) at 37^{o}C in 5% CO_2 incubators. Cells were grown as monolayers in 75 cm^2 flasks at 37˚C and 5% CO_2 and subcultured twice a week or every 3 days. For subculturing the cells, the exhausted media in the flask was aspirated and the confluent adherent cells were washed once with 10 ml HBSS. To detach the hSERT HEK cells from the flask, 3 ml trypsin-EDTA was added and swirled to cover the cell monolayers, and then 2 ml of the trypsin-EDTA was removed, leaving 1 ml of the trypsin-EDTA in the flask. When the cell monolayer was detached from the flask, 9 ml of complete media was added to the flask to inactivate the trypsin. To remove the media containing trypsin-EDTA, a 10 ml cell suspension was transferred into a 15 ml tube and centrifuged at 1000 rpm for 3-4 minutes. After removing the supernatant, the cell pellet was suspended with 10 ml complete media, and 2 ml of the cell suspension was transferred into a new labeled flask containing 18 ml complete media. The flask was tightly capped and then gently swirled to suspend the cells evenly. The flask was placed in the incubator and the cells were allowed to grow until the next subculture.

A stably-transfected WT hDAT N2A cell line employed in the study was kindly provided by Dr. Margaret E. Gnegy's Laboratory (University of Michigan). The hDAT N2A cells were similarly grown, except OPTI-MEM I media supplemented with 10% fetal bovine serum (FBS), 100 units/ml penicillin, 100 units/ml streptomycin and 100

μg/ml of G-418 was used. For whole-cell experiments, one mL of the transfected cell suspension was distributed within 24 well plates and allowed to incubate until confluent.

SITE-DIRECTED MUTAGENESIS AND CONSTRUCTION OF MUTANT PLASMIDS

The mutated fragments of WT hSERT were generated and amplified by the polymerase chain reaction (PCR) using a Quickchange kit. The following single mutations were introduced into WT hSERT by Ms. Yurong Huang, formally of the Surratt lab: Lys490Thr, Glu494His, Glu494Thr, Trp103Ala, Val489Phe and Glu493Asp. The sequences of forward and reverse primers designed for Lys490Thr of hSERT were respectively: 5'-CATACTCCTCCAGCAGCGTCACCACGTAGGCCCCTC-3' and 5'-GAGGGGCCTACGTGTGACGCTGCTGGAGGAGTATG-3'. The sequences of primers designed for Glu494Thr of SERT were: 5'-GCGGGCCCCGTGGATACGTCTCCAGCAGCTTCAC-3' and 5'-GTGAAGCTGC TGGAGACGTATGCCACGGGGCCCGC-3'. The sequences of primers designed for Glu494His of SERT were: 5'-GCGGGCCCCGTGGATAATGCTCCAGCAGCTTCAC-3' and 5'-GTGAAGCTGCTGGAGCATTATGCCACGGGGCCCGC-3'. The sequences of primers designed for Trp103Ala of SERT were: 5'-GACCTGG GCAATGTCGCGCGCTTCCCCTAC-3' and 5'-GTAGGGGAAGCGCGCGACATTGCCCAGGTC-3'. The sequences of primers designed for Val489Phe of SERT were: 5'-GAGGGGCCTACGTGTTCAAGCTGCTGGAGGAG-3' and 5'-CTCCTCCAGCAGCTTGAACACGTAGGCCCCTC-3'. The sequences of primers

designed for Glu493Asp of SERT were: 5'-GTGGTGAAGCTGCTGGACGAGTATGCCACG-3' and 5'-CGTGGCATACTCGTCCAGCAGCTTCACCAC-3'. The primers were synthesized with PAGE purification by Operon (Huntsville, AL). WT hSERT in pcDNA3 vector was used as the template DNA. The reaction tubes were prepared with 40 uL sterile water, 5 uL 10X Pfu reaction buffer, 1 uL WT SERT template (10 ng/uL), 1 uL Primer f (11 uM), 1 uL Primer r (11 uM), 1 uL dNTP, and 1 uL Pfu Turbo polymerase (2.5 U/uL). The reaction was set for 25 cycles with denaturation of the double stranded template DNA at 95˚C for 45 seconds, annealing of the primers to the single stranded DNA at 55˚C for 45 seconds and extension of the new DNA strand at 72˚C for 2 minutes. Agarose gel electrophoresis was employed to confirm that PCR products were of appropriate size. The PCR product was first transformed into MC1061 cells by the heat shock transfection method, followed by plating the cells on ampicillin supplemented agar petri plates and incubating at 37˚C for 16-18 hours. Bacterial colonies were picked to inoculate in 5 ml of LB broth and the bacteria were allowed to grow at 37˚C for 16 hours. The supercoiled plasmid DNA was extracted using Stratagene mini-prep kits. The size of the DNA was screened by agarose gel electrophoresis, and then the mutation-containing region was confirmed by DNA sequencing (University of Pittsburgh core facility). After sequence confirmation, the DNA product containing the mutated region was further chosen to inoculate 200 ml of LB broth to produce large amounts of the cDNA plasmid of interest. The concentration of the cDNA plasmid was assessed by measuring the absorbance at 260 and 280 nm. Plasmid cDNA with a 260/280 ratio of no less than 1.70 was considered pure enough for transient transfection of mammalian cells. The entire

coding sequence of the mutant cDNA plasmid was confirmed by DNA sequencing not to have extraneous mutations.

CELL TRANSFECTIONS

Transient transfections of N2A cells were conducted via the modified calcium phosphate method (Graham and van der Eb, 1973). The day before the transfection, cells were subcultured and incubated in 24-well tissue culture plates (uptake assay) or the 150×10 mm cell culture dishes (ligand binding assay) at 37˚C and 5% CO_2. On the day of transfection, N2A cells were 30-40% confluent. Four hours prior to transfection, the media in the wells was replaced with fresh complete media. To begin the transfection, two sterilized tubes were prepared containing equal volumes of transfection reagents. Millipore water, plasmid DNA, 10X Tris-EDTA (TE) buffer pH 8.0 and 0.5 M $CaCl_2$ were added into the first tube and the concentration of plasmid DNA was diluted to be 14.28 ng/µl. The second tube contained 2X HBS buffer. The contents of the first tube were added into the second tube dropwise with continuous gentle vortexing. Fifty seconds after adding the last drop, a uniform suspension was performed by pipetting the mixture up and down, and the particle size of the DNA complexes was therefore reduced. One hundred µl of the above mixture was then added into each well and the plates were gently swirled to ensure uniform distribution. After 16-18 hours, the media containing Ca^{2+} and unincorporated DNA was replaced with 1 ml fresh complete media. The N2A cells transiently expressing hSERT or hSERT mutations were ready for pharmacological testing by the next day.

COMPETITION BINDING ASSAYS

The cocaine analog [^{125}I]-RTI-55 has been demonstrated to be a useful SERT ligand for the competition binding assays employed here (Boja et al., 1992; Mortensen et al., 2001; Henry et al., 2006b). [^{125}I]-RTI-55 inhibition binding assays performed with HEK cells stably expressing hSERT and N2A cells transiently expressing hSERT constructs were on 150 x 25 mm tissue culture-treated Petri plates. For preparing the cell membrane, cell monolayers were washed 2 x 10 ml with ice-cold phosphate-buffered saline (PBS) and subsequently transferred to 15 ml centrifuge tubes. Following low speed centrifugation, 700 x g, supernatant was aspirated and the cell pellet was resuspended in ice-cold TE buffer (50 mM Tris, pH 7.5, 1mM EDTA). The suspension was subjected to high voltage ultrasonic treatment for 10 seconds to disrupt the intact cells. Homogenate was transferred to cold 1.5 ml microcentrifuge tubes and centrifuged at 100,000 x g at 4˚C for 30 min (Sorvall Discovery M150 centrifuge). Supernatant was aspirated, and the pellet was then resuspended in ice-cold binding buffer (50 mM Tris, pH 7.5, 100mM NaCl). A portion of each sample was quantitated for protein content using the Bradford protein assay. For further performing of the binding assays, [^{125}I]RTI-55 (0.1 nM final concentration), nonradioactive competitor (1 fM~1 μM final concentration), binding buffer, and membrane suspension were combined in 12 x 75 mm borosilicate glass tubes and incubated at room temperature for 1 hour with gentle mixing (orbital shaker). The mixtures were rapidly filtered through glass fiber filters (Schleicher and Schuell, Keene, NH) presoaked in 0.5% polyethylenimine solution (v/v). The filters were washed twice with 5 ml cold 50 mM Tris buffer and transferred to the counting vials. Incorporation of radioactivity was determined using a Beckman scintillation

counter. Non-specific binding was determined by using 1 μM paroxetine. Ki values were determined via nonlinear regression analysis with GraphPad Prism 5.0.

Whole-cell binding experiments used a stable HEK cell line expressing the serotonin transporter. Cells were plated as monolayers in 24-well plates. The cells were washed twice with 2 mL KRH buffer. [^{3}H]-serotonin and increasing concentrations of the nonradiolabeled competitor is added in duplicate to the monolayer of HEK hSERT cells. The incubation proceeded for 15 minutes before washing the monolayer twice with 2 mL of KRH and 500 μL SDS. Cells were then transferred to scintillation vials for determination of the amount of [^{125}I]-RTI-55 able to compete with the nonradiolabeled inhibitor. Nonspecific binding is determined by addition of 10 μM paroxetine. The raw data will be of the specific activity (Ci/mmol) will be determined with GraphPad Prism 4 software.

Separate competition binding assays employed the cocaine analog [^{3}H]-WIN 35,428 as the radiotracer. WT hDAT N2A cell monolayers, in 24-well plates, were washed 2 x 1 ml with KRH/AA buffer (25 mM HEPES, pH 7.3, 125 mM NaCl, 4.8 mM KCl, 1.3 mM $CaCl_2$, 1.2 mM Mg_2SO_4, 1.2 mM KH_2PO_4, 5.6 mM glucose). The cell monolayers were incubated with 500 μl of [^{3}H]-WIN 35,428 (1 nM) and nonradioactive competitor (0.1 nM – 10 μM) for 15 minutes, followed by washing the cell monolayers 2 x 1 ml with KRH/AA buffer. The non-specific binding was determined by using 10 μM mazindol as the blocker. Cell monolayers were solubilized by incubating with 1 ml of 1% SDS at room temperature for 1 hour with gentle shaking. The cell lysates were transferred into scintillation vials containing 5 ml of ScintiSafe fluid and the incorporated

radioligand was determined by employing a liquid scintillation counter. Ki values were analyzed with GraphPad Prism 5.0.

[^{3}H]-SEROTONIN UPTAKE INHIBITION ASSAYS

[^{3}H]-serotonin uptake assays were performed with N2A cells transiently expressing WT hSERT or hSERT mutations or were performed with HEK cells stably expressing hSERT in 24-well plates. For performing uptake assays, cell monolayers were washed 2 x 1 ml with KRH/AA buffer. The cell monolayers were incubated with 375 µl of KRH/AA buffer (total uptake) or 10 µM paroxetine (non-specific uptake) for 10 minutes, followed by incubation with 125 µl of 10 nM [^{3}H]-serotonin for an additional 5 minutes. Cell monolayers were washed 2 × 1 ml with KRH/AA buffer, and then solubilized by incubating in 1 ml of 1% SDS with gentle shaking at room temperature for at least 1 hour. The cell lysates were transferred into scintillation vials containing 5 ml of ScintiSafe fluid, and the incorporated radioligand [^{3}H]-serotonin was determined by employing a liquid scintillation counter. The non-specific uptake was determined by using 10 µM paroxetine if S-citalopram was the blocker or 10 µM S-citalopram if paroxetine was the blocker. The specific uptake was determined by the difference between total and non-specific uptake.

[^{3}H]-DOPAMINE UPTAKE INHIBITION ASSAYS

All [^{3}H]-dopamine uptake assays were performed similar to the [^{3}H]-serotonin uptake assays except 10 nM [^{3}H]-dopamine was used in place of [^{3}H]-serotonin, and the cells were incubated with 375 µl of KRH/AA buffer and the inhibitor (0.1 nM~10 µM)

for 10 minutes, followed by incubation with 125 µl [^{3}H]-dopamine for an additional 5 minutes. The non-specific uptake was determined by using 10 µM mazindol as the blocker. The IC_{50} values for [^{3}H]-dopamine uptake inhibition were determined using GraphPad Prism 5.0.

DATA ANALYSIS

GraphPad Prism 5.0 was used to determine statistical significance using Student's T-test.

MATERIALS AND EQUIPMENT

FACILITIES

Laboratories- Room 456, 414, 408, 457 and 459, Mellon Hall of Science, Duquesne University

MATERIALS

Cell lines

N2A (murine neuroblastoma) cells

Dr.Margaret E. Gnegy's laboratory, Department of Pharmacology, University of Michigan, MI

hSERT HEK cells (HEK cells stably expressing human serotonin transporter)

hDAT N2A cells (N2A cells stably expressing human dopamine transporter)

Dr. Margaret E. Gnegy's laboratory, University of Michigan, MI

hNET HEK cells (N2A cells stably expressing human norepinephrine transporter)

Chemicals and drugs

[^{3}H]-Dopamine (3, 4-[Ring-2, 5, 6-^{3}H]-Dihydroxyphenylethylamine)

Perkin Elmer, Foster City, CA

[^{3}H]-Citalopram

Perkin Elmer, Foster City, CA

[^{3}H]-Paroxetine

Perkin Elmer, Foster City, CA

[^{3}H]-WIN 35,428 ([N-Methyl-^{3}H]-WIN 35,428)

Perkin Elmer, Foster City, CA

[^{3}H]-Serotonin (5-[1, 2-3H(N)]-Hydroxytryptamine creatinine sulfate)

Perkin Elmer, Foster City, CA

[^{125}I]-RTI-55

Perkin Elmer, Foster City, CA

Acetic acid

Fisher Scientific, Pittsburgh, PA

Agarose

Invitrogen Corporation, Carlsbad, CA

Ampicillin sodium salt

Acros, Carlstadt, NJ

Calcium chloride

Sigma-Aldrich Corporation, St. Louis, MO

S-citalopram hydrochloride

Tocris Bioscience, Ellisville, MO

Compressed carbon dioxide

Air Products, Pittsburgh, PA

D-(+)Glucose

Sigma-Aldrich Corporation, St. Louis, MO

Dimethylsulfoxide (DMSO)

Sigma-Aldrich Corporation, St. Louis, MO

Dulbecco's Modified Eagle Medium (DMEM)

Hyclone, Logan, UT

dNTP mix

Stratagene, La Jolla, CA

EDTA

Sigma-Aldrich Co., St. Louis, MO

Ethanol, 200 proof

PharmacoProduct Inc., Brookfield, CT

Ethanol, HPLC grade

ACROS, Fair Lawn, NJ

Ethidium bromide

Fisher Scientific, Pittsburgh, PA

Fetal bovine serum

Hyclone, Logan, UT

G-418 sulfate

Clontech Laboratories Inc., Mountain View, CA

L-Glutamine

Invitrogen, Carlsbad, CA

HEPES free acid

MP Biomedicals Inc., Solon, OH

HBSS/Modified

Hyclone, Logan, UT

Isopropanol (DNase, RNase and protease free)

Fisher Scientific, Pittsburgh, PA

LB agar

Fisher Scientific, Pittsburgh, PA

LB broth

Fisher Scientific, Pittsburgh, PA

Methanol, HPLC grade

Fisher Scientific, Pittsburgh, PA

MC1061 cells

Invitrogen, Carlsbad, CA

Opti-MEM 1

Invitrogen, Carlbad, CA

Paroxetine hydrochloride

Toronto Research Chemicals Inc., North York, ON Canada

Penicillin-Streptomycin

Gibco-BRL, Grand Island, NY

Polymerase, Pfu Turbo

Stratagene, La Jolla, CA

Potassium chloride

Sigma-Aldrich Co., St. Louis, MO

Potassium phosphate, monobasic

Sigma-Aldrich Co., St. Louis, MO

Custom oligonucleotide primers

Operon, Huntsville, AL

RNase A (DNase free)

Fisher Scientific, Pittsburgh, PA

SOC media

Invitrogen, Carlsbad, CA

ScintiSafe scintillation fluid

Fisher Scientific, Pittsburgh, PA

Sodium chloride

Sigma-Aldrich Co., St. Louis, MO

Sodium hydroxide

Fisher Scientific, Pittsburgh, PA

Sodium hydroxide solution

Fisher Scientific, Pittsburgh, PA

Sodium lauryl sulfate

Sigma-Aldrich Co., St. Louis, MO

Tris-EDTA buffer (DNase, RNase and protease free)

Acros, Carlstadt, NJ

Trizma buffer, free base

Fisher Scientific, Pittsburgh, PA

Tris buffer, HCl salt

Sigma-Aldrich Co., St. Louis, MO

Trypsin-EDTA 10X

Gibco-BRL, Grand Island, NY

Tropolone

Sigma-Aldrich Co., St. Louis, MO

Kits

Gel extraction kit

Qiagen Inc., Valencia, CA

PCR purification kit

Qiagen Inc.,Valencia, CA

Plasmid miniprep kit

Stratagene, La Jolla, CA

Plasmid purification kit

Qiagen Inc.,Valencia, CA

Quickchange Mutagenesis kit

Stratagene, La Jolla, CA

Other Materials

Cell culture flasks, 75 cm^2

Corning Inc., Teterboro, NY

Cell culture grade water

Hyclone, Logan, UT

Cell culture plates (10, 25 cm)

Fisher Scientific, Pittsburgh, PA

Centrifuge tube, 15 ml

Corning Inc., Horseheads, NY

Centrifuge vials, 1.5 ml

Corning Inc., Horseheads, NY

Culture tubes, disposable

Fisher Scientific, Pittsburgh, PA

Falcon tubes, 14 ml

Fisher Scientific, Pittsburgh, PA

Falcon tubes, 50 ml

Fisher Scientific, Pittsburgh, PA

Filter unit, sterile

Millipore, Billerica, MA

Eppendorf microcentrifuge tubes, 1.5 ml

Fisher Scientific, Pittsburgh, PA

Parafilm

Fisher Scientific, Pittsburgh, PA

Pasteur pipettes, disposable

Fisher Scientific, Pittsburgh, PA

Pipette tips, disposable Redi-Tips TM (1, 10, 200, 1000 µl)

Fisher Scientific, Pittsburgh, PA

Polaroid film

Fisher Scientific, Pittsburgh, PA

Polypropylene tubes

Fisher Scientific, Pittsburgh, PA

Respirator

Fisher Scientific, Pittsburgh, PA

Scintillation vials

Fisher Scientific, Pittsburgh, PA

Serological pipettes, sterile disposable (5, 10, 25 ml)

Fisher Scientific, Pittsburgh, PA

Syringes, sterile (10 ml)

Fisher Scientific, Pittsburgh, PA

Thermowell PCR tubes

Corning, Horseheads, NY

Tissue culture plates, sterile (6 well, 24 well)

Fisher Scientific, Pittsburgh, PA

Sarstedt Inc., Newton, NC

EQUIPMENT

Analytical balance

Mettler Toledo Inc., Columbus, OH

Cell culture incubator

Forma Scientific, Worcester, MA

Centrifuge, Model 228

Fisher Scientific, Pittsburgh, PA

Refrigerated tabletop centrifuge, Model 5810R

Eppendorf Scientific, Hauppauge, NY

Eppendorf dispenser (50 ml)

Brinkmann Instruments Inc., Hauppauge, NY

Electrophoresis power supply

Life Technologies Inc., Gaithersburg, MD

Horizontal gel electrophoresis system

Life Technologies Inc., Gaithersburg, MD

Isotemp incubator

Fisher Scientific, Pittsburgh, PA

Lab freezers and refrigerators

Forma Scientific, Worcester, MA

Liquid nitrogen tank

Department of Chemistry and Biochemisty, Duquesne University

Liquid Scintillation Analyzer

Packard Instruments, Meriden, CT

Millipore Milli-Q ultrapure water system

Millipore, Billerica, MA

Mixer 37600

Thermolyne Corporation, Duqubue, IA

NapFLOW Laminar air flow unit

Fisher Scientific, Pittsburgh, PA

ORBIT Shaker

Lab-line Instruments Inc., Melrose Park, IL

PCR Mastercycler

Eppendorf Scientific, Hauppauge, NY

pH Meter AB15

Fisher Scientific, Pittsburgh, PA

Pipet-aid

Drummond Scientific Co., Broomall, PA

Pipetman (P-2, P-10, P-20, P-100, P-200, P-1000)

Mettler Toledo Company, Woburn, MA

Polaroid Gelcam

Polaroid Corporation, Cambridge, MA

Universal vacuum system UVS 400

Savant Instrument Inc., Holbrook, NY

UV transilluminator M-26

UVP Inc., Upland, CA

UV-visible spectrophotometer DU 530

Beckman Instruments Inc., Fullerton, CA

Vacuum pressure pump

Barnant Co., Lake Barrington, IL

Vertex-2 Genie vortexer

Scientific Industries Inc., Bohemia, NY

Water bath, 180 series

Precision Scientific, Winchester, VA

Water bath, Iso TEMP 205

Fisher Scientific, Pittsburgh, PA

Microbalance

Denver Instruments Co., Denver, CO

Sorvall ultra centrifuge

Thermo Fisher Scientific, Asheville, NC 28806

COMPUTER SOFTWARE

Adobe Acrobat Reader 7.0

Adobe Systems Inc., San Jose, CA

Adobe Acrobat Writer

Adobe Systems Inc., San Jose, CA

ChemDraw Ultra 11.0

CambridgeSoft Corporation, Cambridge, MA

GraphPad Prism 5.0

GraphPad Software, San Diego, CA

Microsoft Office Word & Excel 2007

Microsoft Corporation, Seattle, WA

Molecular Operating Environment 2005.06/2007.09

Chemical Computing Group, Montreal, Canada

Results

Aim 1 Results

Aim 1 was to characterize SERT inhibitor binding sites using pharmacological testing of known inhibitors and analogs. Analogs of known SERT inhibitors were tested for binding affinities in HEK cells stably expressing hSERT. These analogs were created by the laboratory of Dr. David Lapinsky in an attempt to elucidate contacts made within the proposed binding pocket of the protein. The analogs were derived from 6-nitroquipazine, citalopram, fluoxetine, or a novel compound that used a fusion of 6-nitroquiupazine thought to contribute to neurogenesis (MacMillan et al. 2011). The parent compounds were chosen due to their known binding and specificity to SERT.

The 6-nitroquipazine analogs were coded SADU 2-172 and SADU 2-179. The norfluoxetine analogs were coded DJLDU 3-104, 3-114, and 3-126. The citalopram compounds were coded NYDU 2-58, 2-63, 2-129, and 2-131. The fluoxetine analogs were coded NYDU 2-92 and 2-103. The neurogenesis compounds were coded SADU 3-158 and 3-162. As shown in Table 1, most of the analogs, whether the changes were made to add a specific functional group, a cross-linker, or a radioisotope, showed differences in binding affinities but were still within the nanomolar range when compared to the parent compounds.

COMPOUND	hSERT Ki (nM)
6-nitroquipazine (SADU 2-172)	0.12
SADU 2-179	124.7
Norfluoxetine (SADU 2-191)	26
DJLDU 3-104	102
DJLDU 3-114	65.7
DJLDU 3-126	724.3
Citalopram	4.4
NYDU 2-58	1.46
NYDU 2-63	4.3
NYDU 2-129	<1
NYDU 2-131	6.7
Fluoxetine (SADU 3-89)	4.4
NYDU-2-92	161.3
NYDU 2-103	771
P7C3 (MacMillan Neurogenesis)	N/A
SADU 3-158	11.13
SADU 3-162	4.74

Table 1: Binding affinities of SERT inhibitors and analogs at HEK cells stably expressing hSERT. Compounds are color-coded to group parent compounds with analogs.

For consistency in a laboratory setting, it is important to standardize the conditions for experiments. These conditions include the amount of protein used in a ligand-protein binding experiment. In order to standardize the conditions for SERT membrane pharmacology, optimization experiments were carried out via saturation binding of cocaine or clomipramine, a TCA, binding. Drug preincubation time was altered with no effect on hSERT binding. Alternatively, the dilution of the membrane solution, which was done using membrane binding buffer, made a difference in the final Ki values obtained from the saturation binding assays (Figure 4). This difference is important for consistency of current and future experiments, as it alters the level of protein available to bind to the available ligand. As the dilution of 1/16 resulted in affinity values closest to reported clomipramine values of 0.3 nM (Goodman & Gilman, 2011), this was chosen as the optimized membrane dilution for the binding assay method.

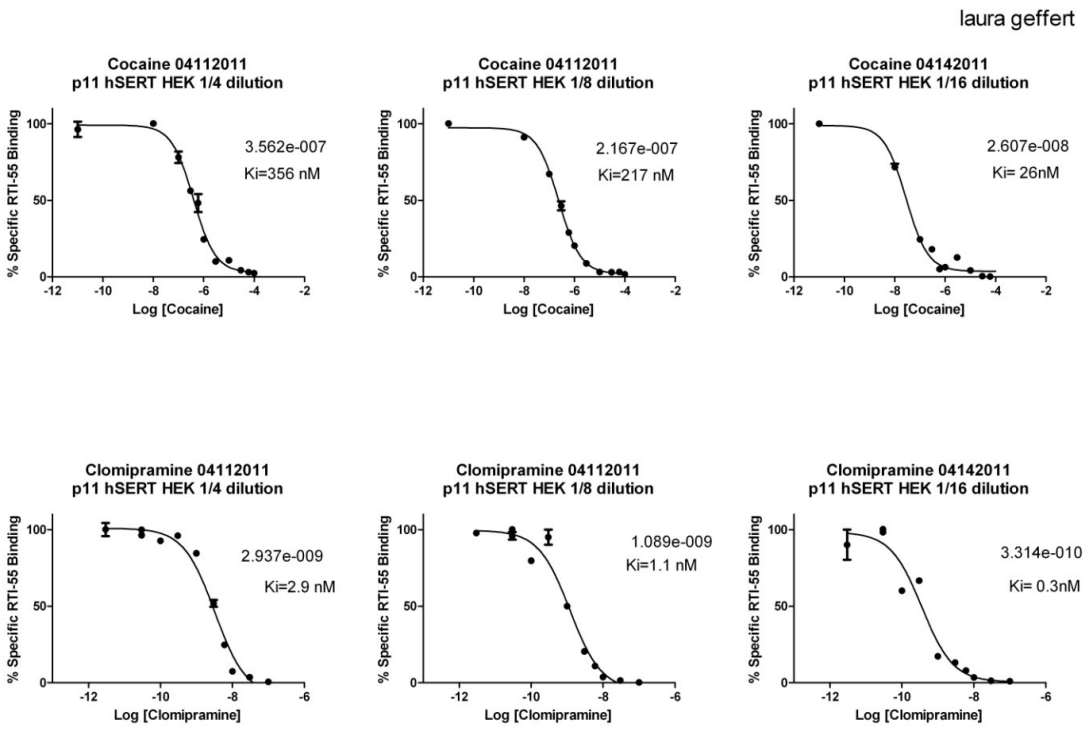

Figure 4: hSERT HEK293 membrane concentration optimization via saturation binding of cocaine or clomipramine.

Aim 2 Results

Aim 2 was to use a SERT model to identify logical mutagenesis targets for *in vitro* characterization. Competition binding assays and uptake assays used N2A cells transiently transfected with a cDNA encoding the wildtype (WT) or mutant SERT protein. These assays measured binding affinity or [3H]-serotonin uptake inhibition potency (SUIP) of established SERT ligands at each SERT mutant relative to that of WT SERT. SERT mutants created by Yurong Huang were W103A, V489F, K490T, E493D, E494H, and E494T. Naïve N2A cells were used as the negative control. Cells transfected with a SERT mutation may show a change in ligand affinity. A decrease or elimination of ligand affinity for a mutated SERT protein would indicate an important binding role for the substituted amino acid. A decrease in function due to a change in a specific amino acid could suggest the location of a binding pocket, but it could also simply imply the amino acids importance in the structural configuration of the SERT protein.

Inhibitor binding screening by WT SERT and mutants shows significant increase in radioligand binding by W103A mutant

Screening of binding affinities at WT SERT and the mutants transiently transfected into N2A cells were done in order to evaluate changes to their ability to bind known inhibitors. As shown in Figure 5, [^{125}I]-RTI-55 binding to W103A was significantly increased as compared to [^{125}I]-RTI-55 binding at WT SERT.

Uptake inhibitor screening at WT or mutant SERT shows a significant decrease in [^{3}H]-serotonin uptake by W103A, V489F, K490T, E494H, and E494T mutants

Screening of uptake capacities for WT SERT and the mutants transiently transfected into N2A cells were done in order to evaluate potential changes in transporter function. As shown in Figure 5, a decrease in [^{3}H]-serotonin uptake was seen at W103A, V489F, K490T, E494H, and E494T, but not at E493D.

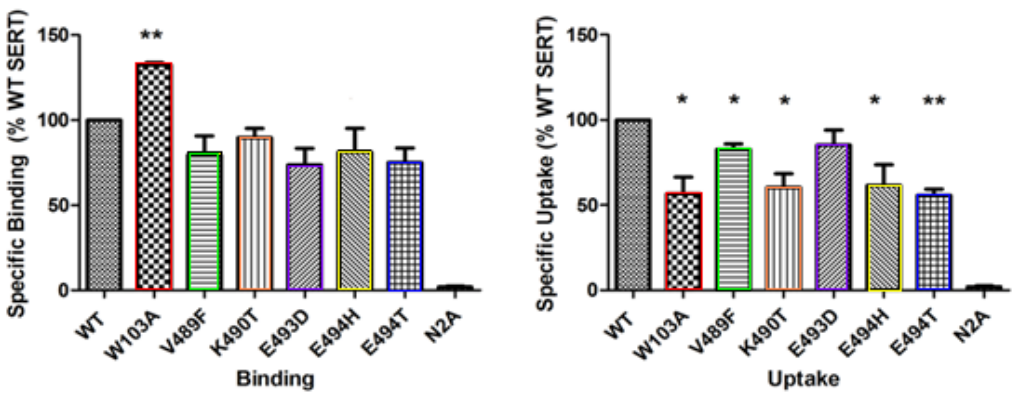

Figure 5: Screening for inhibitor binding and substrate uptake at hSERT mutants transiently expressed in N2A neuroblastoma cells. *p<0.05, **p<0.01.

Binding and uptake assays were performed using N2A cells transiently transfected with WT SERT or a mutated construct. Non-radioactive RTI-55, citalopram, sertraline and cocaine were used in the assays as SERT inhibition competitors. [^{125}I]-RTI-55 was used as the radioactive competitor in the binding experiments, and [^{3}H]-serotonin was used in the uptake inhibition experiments. Binding and uptake results with the mutants are presented in Table 2.

W103A mutation had no effect on binding affinities, but increased uptake inhibition of citalopram

Although the inhibitor binding screening only showed a significant difference between WT SERT and W103A (Figure 5), no changes occurred for any of the inhibitor binding affinities with W103A (Table 2). SSRI serotonin uptake inhibition potency increased as much as 6-fold with the TM1 W103A mutation. Net specific [^{3}H]-serotonin uptake at W103A fell approximately 2-fold even though B_{max} value for [^{125}I]-RTI-55 saturation binding was not significantly affected.

V489F mutation increased binding affinity to RTI-55, but decreased to cocaine, and increased uptake inhibition of citalopram

Affinity for the cocaine analog RTI-55 increased 2-fold at the V489F mutant, but cocaine binding affinity decreased by 2-fold. Based on the structural differences between cocaine and its analog RTI-55, it can be suggested that the TM10 V489 residue may be in the vicinity of the C-3 tropane substituent of each drug. Citalopram but not sertraline potency increased 2-fold with the V489F substitution.

K490T mutation increased binding affinity to RTI-55

Affinity for the cocaine analog RTI-55 increased 2-fold at the V489F and K490T mutants. Binding affinities to citalopram, sertraline, and cocaine were unaffected with the mutation, as well as the uptake capacities.

E493D mutation decreased binding affinity to citalopram, sertraline, and cocaine, and decreased uptake inhibition of citalopram and sertraline.

Citalopram binding affinity decreased 3-fold and sertraline affinity decreased 7-fold with the conservative E493D substitution. Although SSRI serotonin uptake inhibition potency increased as much as 6-fold with the TM1 W103A mutation, potency decreased 6-fold at the TM10 E493D mutant.

E494H and E494T mutations decreased binding affinity to citalopram, and E494H decreased uptake inhibition of citalopram

Citalopram binding affinity decreased 3-fold at E494H and by over 2-fold at E494T, but citalopram potency decreased 3-fold only at E494H, not at the charge-neutral E494T substitution. Interestingly, sertraline affinity decreased 7-fold with the conservative E493 substitution but was unaffected by the E494 mutations. Because the E493 and E494 side chains are expected to diverge in space, loss of one glutamate side chain should not be compensated for by the presence of the other. Net specific [^{3}H]-serotonin uptake at both E494 SERT mutants fell approximately 2-fold even though B_{max} values for [^{125}I]-RTI-55 saturation binding were not significantly affected. This phenomenon also occurred with the W103A mutant.

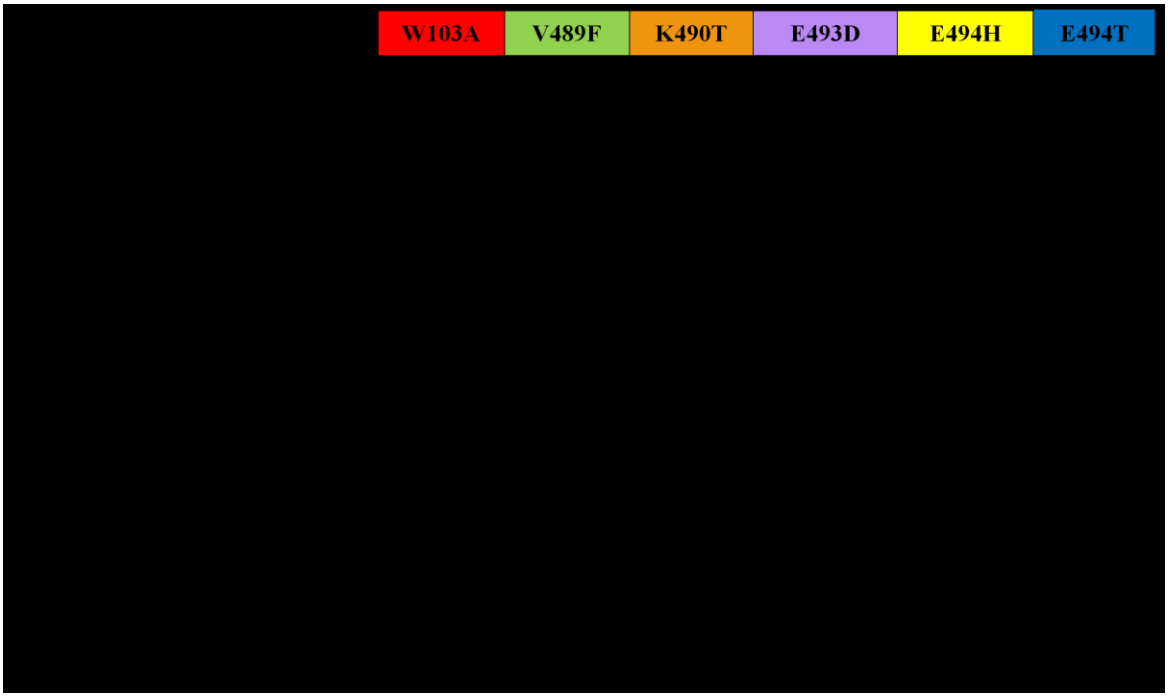

Table 2. Binding affinities & uptake inhibition potencies of SERT inhibitors at N2A neuroblastoma cells transiently expressing wildtype or mutant SERT proteins. *p<0.05, **p<0.01 vs WT. This table, minus the sertraline data, first appeared in the thesis of Yurong Huang, 2011. Some boxes are bold to highlight significant differences of binding or uptake when compared to WT results.

The pharmacological data shown in Table 2 suggest that when mutated singly, no one of the five SERT vestibular pocket residues surveyed is critical for high affinity binding of cocaine or the two SSRIs tested. These results are consistent with similar vestibular pocket SERT mutants (Anderson, 2009). These results were presented at the College on Problems of Drug Dependence conference (Miami, FL, 2011).

Aim 3 Results

Aim 3 was to identify compounds with new structural scaffolds that bind to SERT. One-point binding assays were performed using HEK cells expressing hSERT with fourteen of the top hit compounds (LM series) from the SERT model created by Dr. Martin Indarte (referred to as the MI SERT model). [^{125}I]-RTI-55 was used as the radioactive competitor in the binding experiments. One-point binding assays using clomipramine was performed as positive control and buffer as negative control and total [^{125}I]-RTI-55 binding. Results are presented as the percentage of competing radioligand binding with the hit compound.

Hit compounds from MI SERT model did not inhibit [^{125}I]-RTI-55 binding

As seen collectively in Figure 6, none of the compounds screened as "hits" from the MI model inhibited [^{125}I]-RTI-55 binding at SERT more than the arbitrarily-set threshold of 50%. This threshold was set as a standard guidepost based on the high concentration of drug (10μM) used to compete with [^{125}I]-RTI-55 binding.

Using the *in silico* model created by Dr. Sankar Manepalli (referred to as the SM SERT model), two sets of compounds were chosen for pharmacological testing. The first set, SM, were higher ranking in silico than the MS set, and tested first. One-point binding assays were performed using HEK cells expressing hSERT, hDAT, or hNET with the hit compounds from the SM series from the MI SERT model. [^{125}I]-RTI-55 was used as the radioactive competitor in the binding experiments. Results are presented as the percentage of competing radioligand binding with the hit compound.

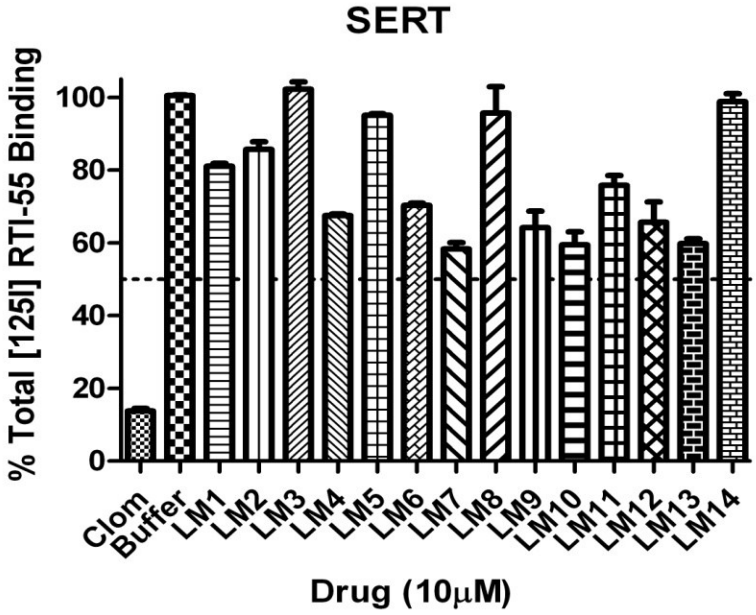

Figure 6: One-point binding of compounds in LM series to SERT

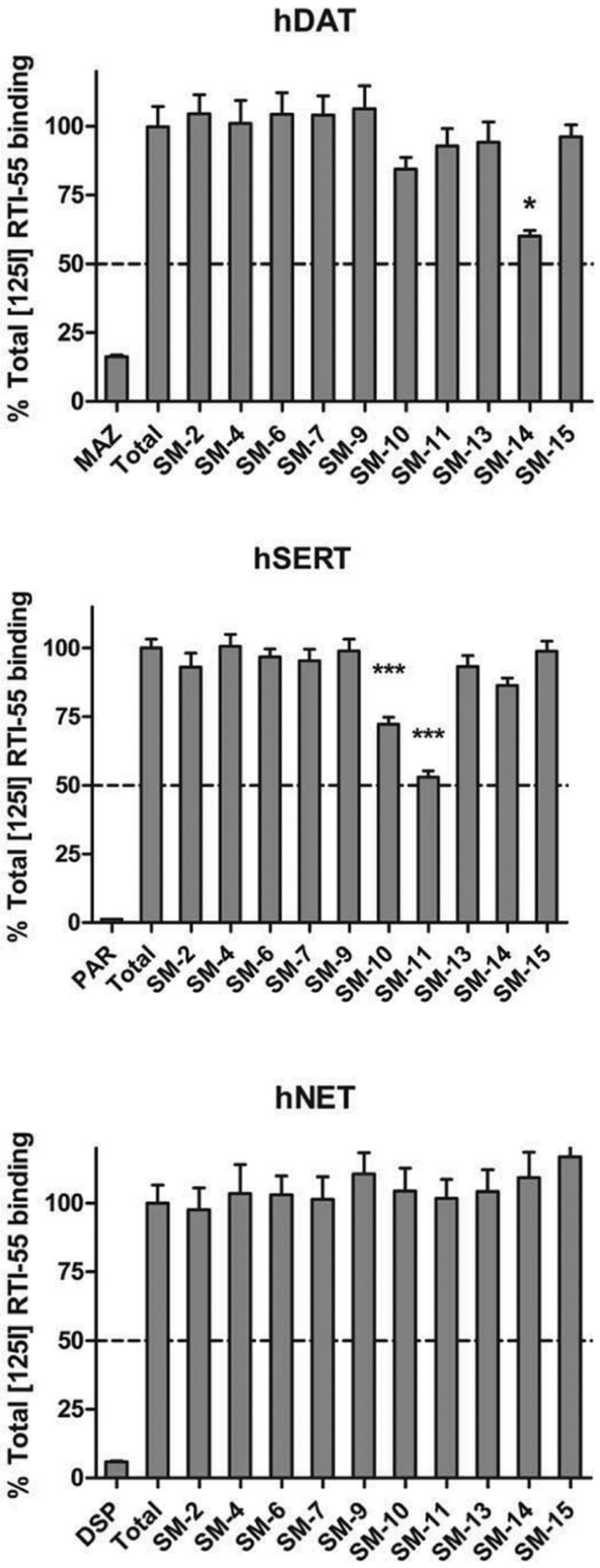

Figure 7: One-point binding of compounds in SM series to SERT

Hit compounds from SM series of SM SERT model did not inhibit [^{125}I]-RTI-55 binding at hNET

A set of hit compounds screened at the SM SERT model was acquired and pharmacologically tested in one-point binding assays at hNET. As seen collectively in Figure 7, none of the SM series compounds screened as "hits" from the SM model significantly inhibited [^{125}I]-RTI-55 binding at HEK cells expressing hNET.

One compound from SM model inhibited [^{125}I]-RTI-55 binding at hDAT

A set of hit compounds screened at the SM SERT model was acquired and pharmacologically tested in one-point binding assays at hDAT. Nine of the ten compounds showed no significant binding affinity to HEK cells expressing hDAT. Although SM14 displayed no significant binding to hSERT, it appeared to inhibit [^{125}I]-RTI-55 binding to hDAT by 40%. Binding and uptake assays were completed and established an average Ki of 15.6 ± 2.4 μM and IC50 of 10.5 ± 4.6 μM (Figure 8).

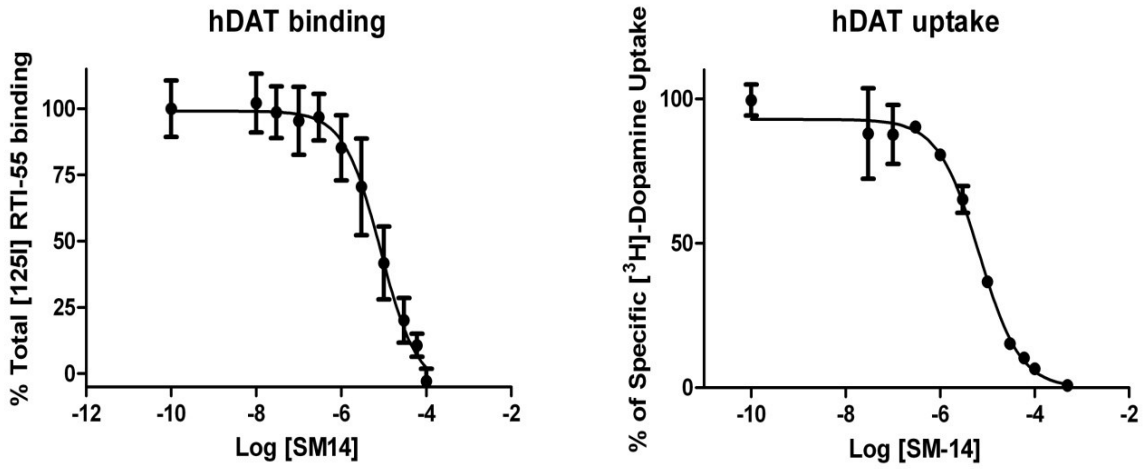

Figure 8: Saturation binding and uptake of VS hit compound SM14 at hDAT HEK293 cells.

Two compounds from SM model inhibited [^{125}I]-RTI-55 binding at SERT

A set of hit compounds screened at the SM SERT model was acquired and pharmacologically tested in one-point binding assays using HEK cell expressing hSERT. Two of the compounds screened using the SM model from the SM series, coded SM10 and SM11, were found to have selective affinity for SERT over the dopamine transporter and norephinephrine transporter (Figure 7). The structures of these two compounds are seen in Figure 9.

SM10 and SM11 were used in a saturation binding experiment for [^{125}I]-RTI-55 inhibition. SM10 was found to have an inhibition constant (Ki) equal to 38 ± 17 μM. The Ki value for SM11 was found to be 17 ± 7 μM (Figure 9).

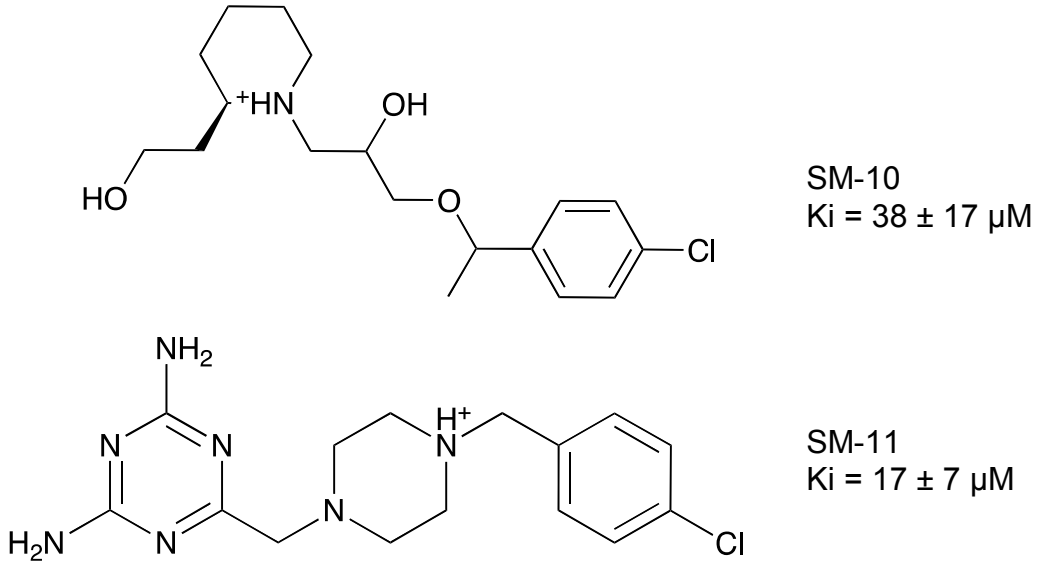

Figure 9: Structures of two VS hit compounds showing affinity for SERT. Reprinted with permission from Manepalli, S., Geffert, L.M., Surratt, C.K., Madura, J.D. (2011). Discovery of novel selective serotonin reuptake inhibitors through development of a protein-based pharmacophore. *J Chem Information and Modeling. 51;* 2417-2426. Copyright 2011 American Chemical Society.

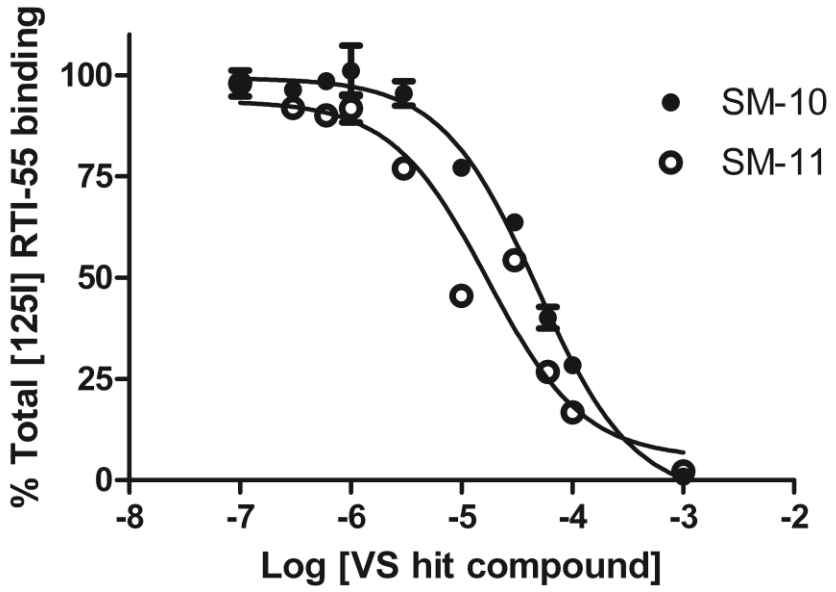

Figure 10: Saturation binding of VS hit compounds SM10 (closed circles) and SM11 (open circles) at hSERT HEK293 cells. Reprinted with permission from Manepalli, S., Geffert, L.M., Surratt, C.K., Madura, J.D. (2011). Discovery of novel selective serotonin reuptake inhibitors through development of a protein-based pharmacophore. *J Chem Information and Modeling. 51;* 2417-2426. Copyright 2011 American Chemical Society.

These results were published in the Journal of Chemical Information and Modeling (Manepalli, et al., 2011).

Second set of hit compounds from SM SERT model did not inhibit [^{125}I]-RTI-55 binding

A second set of hit compounds from the SM SERT model received lower ranking scores. The compounds were acquired and pharmacologically tested in one-point binding assays at hSERT. As seen collectively in Figure 11, none of the MS series compounds screened as "hits" from the SM model inhibited [^{125}I]-RTI-55 binding at SERT more than the arbitrarily-set threshold of 50%.

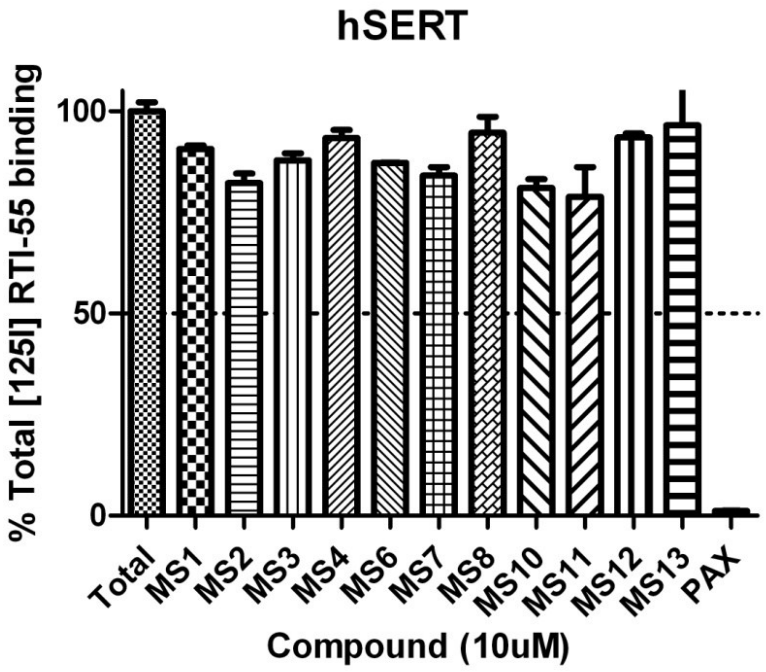

Figure 11: One-point binding of compounds in MS series to SERT

Discussion

The SERT and other monoamine transporters have not yet been crystallized, but membrane protein structures can be studied using a variety of techniques. Developing a computation model of the serotonin transporter (SERT) has been important for the modeling field and for the monoamine field. A model can be an important tool for the molecular dissection of certain structure function activities or ligand-protein interactions. A useful model opens up new possibilities for the development of possible new antidepressants as well as prepare the field for the creation and testing of models of other proteins which are not crystallized as of yet. This project demonstrates how an in silico model can be used in the pharmacological sciences and have applications for medicinal chemistry. The aims fulfilled in this study became a possibility when the bacterial leucine transporter (LeuT), which shares with the SERT 25% identity and 45% similarity (Figure 2) at the amino acid sequence level (Beuming et al., 2006), was crystallized (Yamashita et al., 2005). Moreover, based on the sequence similarities, LeuT is thought to have the same mechanism of transport as SERT. This project also provides an innovative perspective into the interactions of monoamine transporters and inhibitors, which can support therapeutic development for disease states associated with SERT, such as depression and anxiety.

As shown in Table 1, most of the analogs created by the laboratory of Dr. David Lapinsky, whether the changes were made to add a specific functional group, a cross-linker, or a radioisotope, showed only modest differences in binding affinities when

compared to the parent compounds. The pharmacologic similarities between the parent drugs and their analogs are encouraging, suggesting physiologic relevance of the latter as surrogates. Although the results are not able to predict functionality, the ability of the analogs to bind to SERT is a positive advancement toward the development of novel therapeutics.

A known SERT compound, 6-nitroquipazine, and an analog coded SADU 2-179 were tested at hSERT. The analog represents a potential photoaffinity ligand. The affinity of the analog for hSERT, albeit high in the nanomolar range, decreased when compared to the parent compound. This change can be attributed to the additional functional group added to the analog, which may be offering a small amount of steric hindrance to binding in the SERT pocket.

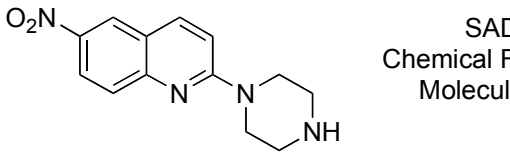

SADU 2-172t9-13
Chemical Formula: $C_{13}H_{14}N_4O_2$
Molecular Weight: 258.28

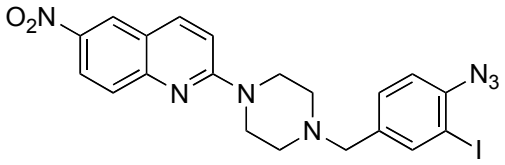

SADU 2-179
Chemical Formula: $C_{20}H_{18}IN_7O_2$
Molecular Weight: 515.31

Figure 12: Structure of 6-nitroquipazine and one analog tested at hSERT.

The norfluoxetine analogs were coded DJLDU 3-104, 3-114, and 3-126. DJLDU 3-104 represents racemic norfluoxetine (Figure 13). DJLDU 3-114 and DJLDU 3-126 represent the S- and R-enantiomer of norfluoxetine respectively. The affinities of DJLDU 3-104 and DJLDU 3-144 were similar to the parent compound, suggesting the enantiomers are likely binding in the same binding pocket. The R-enantiomer, DJLDU 3-126, displayed a lower affinity than the S-enantiomer. This suggests that the structural difference between the analogs allows for either a different binding mode or orientation in the SERT inhibitor pocket. In this way, the use of norfluoxetine analogs can assist in probing biding sites. The structural differences, along with their binding results, could indicate the protein-ligand interactions which are occurring in the proposed binding pocket.

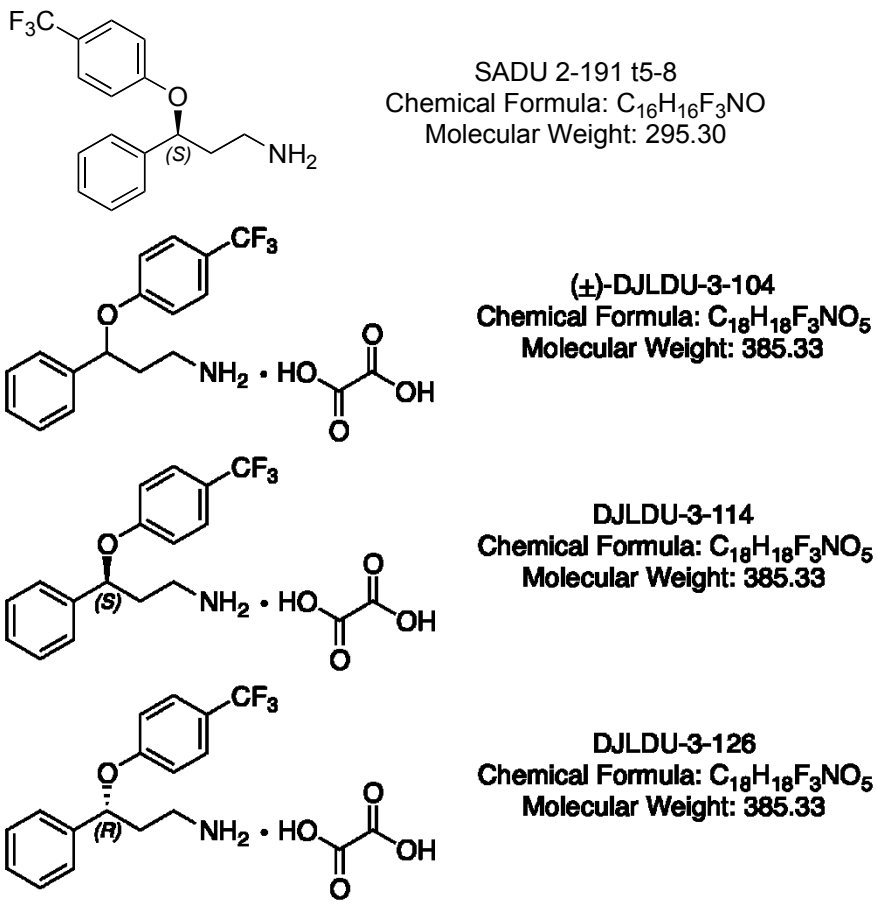

Figure 13: Structures of norfluoxetine (SADU 2-191) and three analogs tested at hSERT.

The citalopram compounds were coded NYDU 2-58, 2-63, 2-129, and 2-131. Citalopram is a compound with a hSERT binding affinity of 4.4 nM. It is not surprising that the analogs were found to have high binding affinities because their parent compound, with a similar structure, also has a high binding affinity. NYDU 2-58 represents citalopram derivatized with an acetophenone photoreactive group and a terminal alkyne clickable handle (Figure 14). Clickable handles are a useful way to connect a new structural addition to a compound using a single chemical reaction. NYDU 2-63 also represents citalopram with a terminal alkyne clickable handle, but has a benzophenone photoreactive group. NYDU2-129 and 2-131 are both enantiomerically pure S-citalopram clickable photoprobes. NYDU 2-131 was tested to see if the bulky benzophenone off of the nitrogen was tolerable for SERT binding. The structural differences between citalopram and its analogs in addition to the binding results, suggest that different binding modes could be occurring for the analogs in the SERT inhibitor binding pocket. In this way, the pharmacological testing of citalopram analogs can assist in probing biding sites and indicate changes to potentially improve on the parent compound.

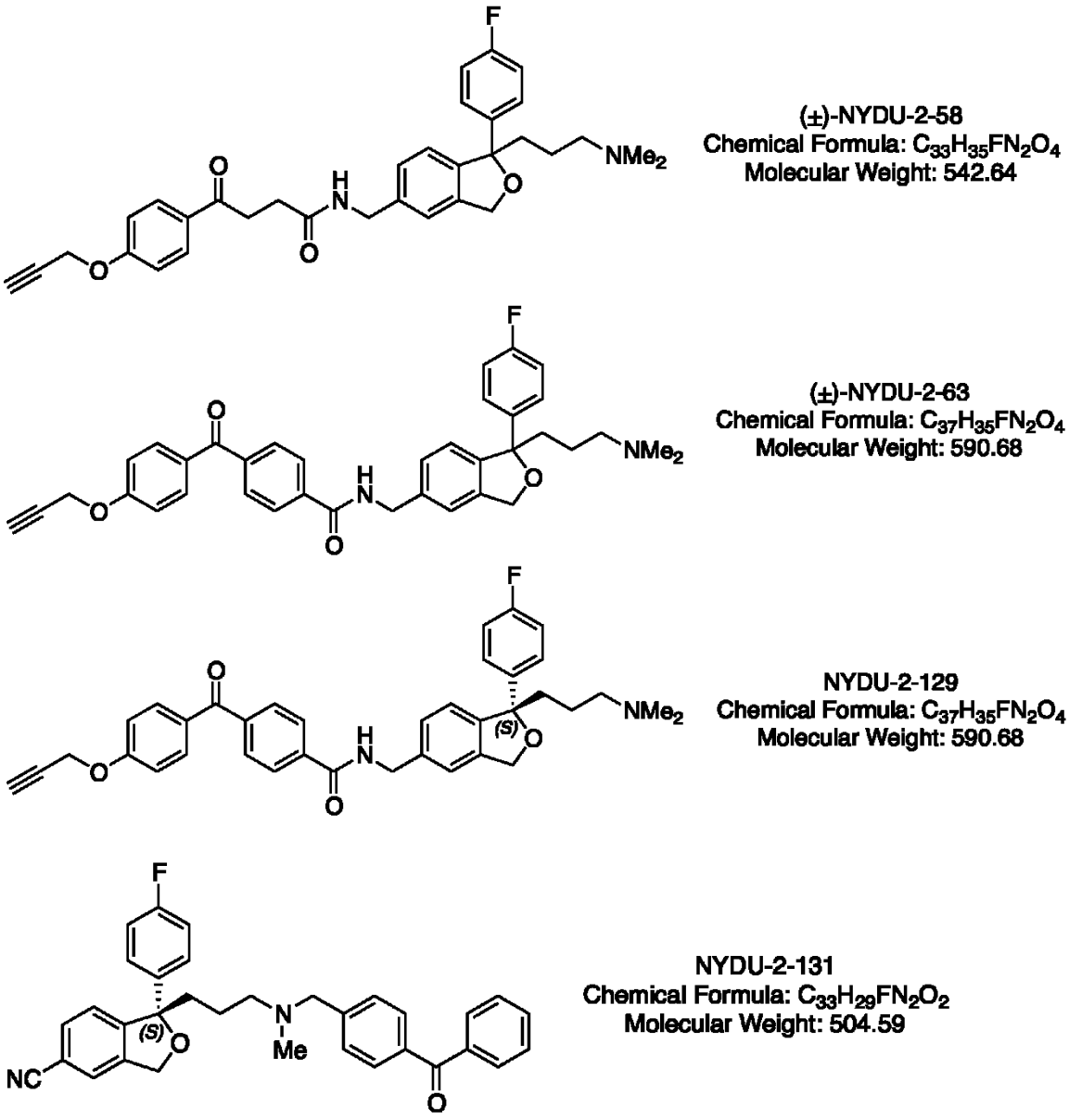

Figure 14: Structures of two citalopram analogs tested at hSERT.

The fluoxetine analogs were coded NYDU 2-92 and 2-103. Both of these compounds represent racemic fluoxetine derivatized with a linker, a photoreactive benzophenone, and a clickable propargyl ether/alkyne handle. The affinity difference between the two analogs could be due to the single structural difference of a methyl group exchanged for hydrogen (Figure 15). Although the fluoxetine analogs did not show improved binding affinity for SERT when compared to the parent compound, the results still aid in probing the proposed binding site and were created to add structures, including the linker, photoreactive benzophenone, and the clickable alkyne handle, to the parent compound for purification and detection. In conclusion, the pharmacological testing of the fluoxetine analogs can indicate protein-ligand interactions in the binding pocket to perhaps be a hydrophobic pocket with favorable interactions near the methyl group of NYDU 2-92.

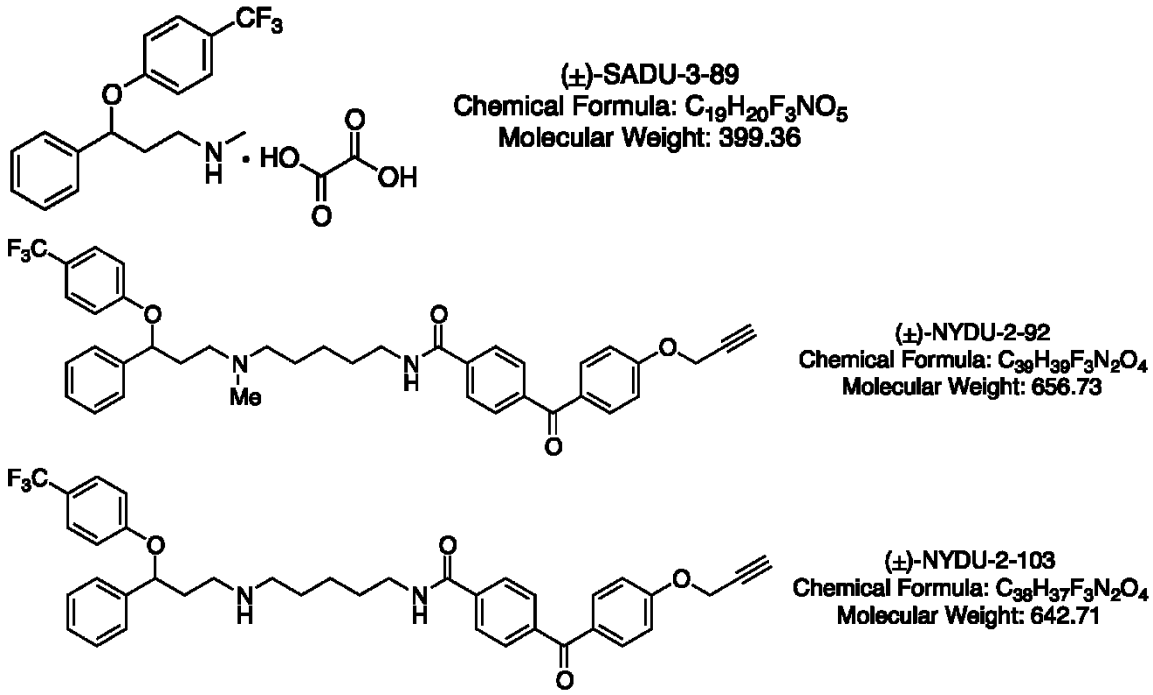

Figure 15: Structures of racemic fluoxetine (SADU 3-89) and two analogs tested at hSERT.

Chronic antidepressant treatment has been shown to increase cell proliferation, increase neuronal survival, and reverse the stress-induced decrease of hippocampal neurogenesis (Alonso et al., 2004). The ability to increase hippocampal neurogenesis is a common feature of both SSRIs and TCAs (Malberg et al., 2000). It is suggested that hippocampal neurogenesis might be a major factor in the action of antidepressants. The neurogenic compounds were coded SADU 3-158 and 3-162. SADU 3-162 is a P7C3 analog with fusion of 6-nitroquipazine. These analogs were created from a parent compound (P7C3) that was found to be proneurogenic and neuroprotective (MacMillan et al., 2011). Unlike some antidepressants that have been reported to enhance neurogenesis after two or three weeks of treatment, P7C3 effects neurogenesis within days of administration. The molecular target of the parent compound is unknown, but the high affinity of compounds SADU 3-158 and 3-162 for hSERT would also make these good candidates for behavioral testing. Multiple tests are commonly used in the field to test the antidepressant properties of compounds, including the tail suspension test, the forced swim test, and the novelty-induced hypophagia test (Talbot, et al., 2010).

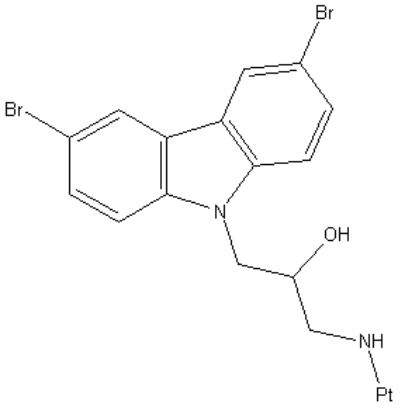

P7C3

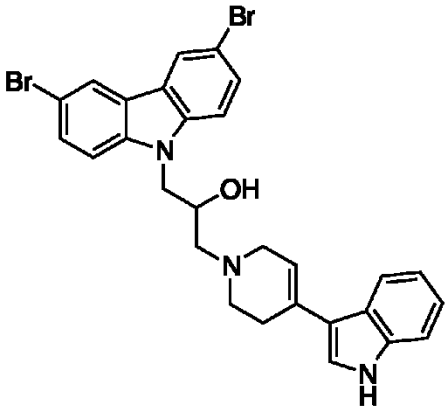

(±)-SADU-3-158
Chemical Formula: $C_{28}H_{25}Br_2N_3O$
Molecular Weight: 579.33

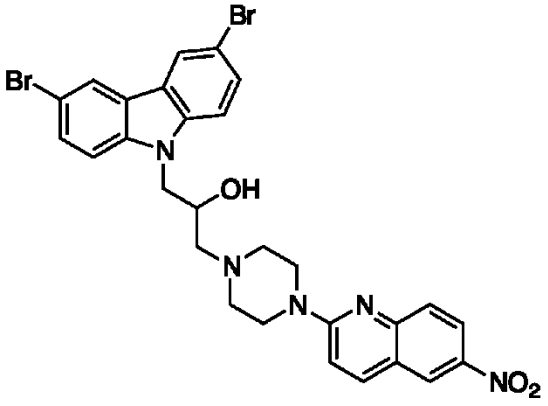

(±)-SADU-3-162
Chemical Formula: $C_{28}H_{25}Br_2N_5O_3$
Molecular Weight: 639.34

Figure 16: Structure of Proneurogenic compound P7C3 (MacMillan et al. 2011) and analogs created by Dr. David Lapinsky. Analogs were tested at hSERT.

In silico models have guided numerous site-directed mutagenesis studies for the purpose of characterizing the ligand-SERT protein interaction (Forrest et al., 2007; Zhou et al., 2009). The importance of specific residues for activity of the transporter can be established using a stable serotonergic cell line and pharmacological assays (Kaufmann et al., 2009). Therefore, the functional significance of different drugs at the transporter site can be predicted using the virtual model of SERT as a rational starting point. Mutagenesis allows a focus on a particular amino acid or group of amino acids to assess their contribution to structure and functional properties, such as binding and uptake. Some studies utilizing *in silico* models have found results consistent with mutagenesis and consistent with the use of pharmacological methods (Andersen et al., 2009; Barker et al., 1998; Beuming et al., 2008). No particular amino acid or sequence has been found to be characteristic of inhibitor binding sites.

Our study aimed to characterize the SERT inhibitor binding sites using pharmacological testing of known inhibitors with rationally-designed SERT mutants. Ms. Yurong Huang, formerly of the Surratt lab, used *in silico* SERT models to guide selection and creation of the mutants (Figures 3). The importance of the replaced amino acid was determined via binding and uptake assays with the mutants transiently expressed in naïve N2A cells.

SERT mutants created and assessed for binding and uptake capacity were W103A, V489F, K490T, E493D, E494H, and E494T. These residues were implicated *in silico* as components of a SERT binding pocket. W103A is found in the first transmembrane domain (TM1) of the SERT protein, while the other mutants are found in the tenth

transmembrane domain (TM10). These particular amino acids were chosen for mutation based on evidence for not only a primary binding pocket for the substrate (interior), but also for a secondary pocket in the vestibular region that may be responsible for substrate and inhibitor binding and overlap between the two pockets (Andersen et al, 2009). The unwinding of TM1 and TM6 exposes main chain carbonyl oxygen and nitrogen atoms, which form a hydrogen bond to the substrate and the sodium ions. The external gate is composed of one arm between TM1 and TM10 and another arm between TM3 and TM8, and binding of the substrate may be governed by the opening and closing of the gate, thereby regulating the binding of inhibitors. If a mutant shows impaired SERT inhibitor binding, it would be consistent with the idea that the endogenous amino acid plays a role in the binding process and would be partial confirmation that the binding pocket was identified. Co-crystals of LeuT with a bound TCA show a salt bridge formed by TM1 and TM10 with a water molecule being displaced (Sinning et al, 2009). TCAs have been thought to bind farther into the vestibule of SERT, causing a rotation of the inhibitor, which would disrupt the salt bridge between Arg104 and Glu493. Further information on the residue in question can be gained by identifying which amino acids restore function at that position (Henry et al, 2005). The discrimination of the drug binding site will aid in the search for novel SERT ligands with high affinity and specificity using in silico models of SERT.

Screening of binding affinities at WT SERT and the mutants transiently transfected into N2A cells were done in order to evaluate potential changes to their ability to bind known inhibitors. Our results of an inhibitor binding screening at WT SERT and the mutants

demonstrated a significant increase at W103A compared to WT SERT, but no change was seen in binding affinities of the other mutants. Screening of uptake capacities for WT SERT and the mutants transiently transfected into N2A cells were done in order to evaluate potential changes in transporter function. Our results of substrate uptake screening at WT SERT and the mutants demonstrated a significant decrease in [^{3}H]-serotonin uptake at W103A, V489F, K490T, E494H, and E494T. This substrate uptake decrease was not seen at the E494D mutation. Generally, these results could indicate that members of the NSS family accommodate the structural and functional differences of substrates by subtle changes in the amino acids present in the substrate binding sites. Therefore, this could signify that changing the glutamic acid at the 494 position to an aspartic acid has no effect on the ability of the transporter to transport serotonin across the membrane.

Interestingly, when mutated singly, no one of the five surveyed SERT inhibitor binding pocket residues is critical for high affinity binding of cocaine or the two SSRIs tested. The binding and uptake profiles of each of the mutants suggest differing roles with respect to substrates and inhibitors within the binding pocket of SERT. The results gained from the screening are important points of reference and provide useful information for the refinement of the model. The known SERT inhibitors used in the mutagenesis studies can be docked into mutant *in silico* SERT models, thus allowing investigators to understand if the orientation of the inhibitor is changing due to the mutation. The complete binding curves and substrate uptake curves present a comprehensive representation of the binding affinities and functionality of the mutants

being tested. The roles and suggested proximities of each amino acid to the SERT binding pocket(s) can impact the search for novel therapeutics. This impact can be the altering of what structures and scaffolds could be used for the desired binding to SERT as well as how a novel therapeutics could interact with other proteins. Unknown interactions of other proteins, such as 5-HT receptors, impact side-effects seen with potential antidepressant.

If a mutant shows impaired SERT inhibitor binding, it would be consistent with the idea that the endogenous amino acid(s) plays a role in the binding process and would be partial confirmation that the binding pocket was identified. Prior mutants which were assessed for binding and uptake capacity were W103A, V489F, K490T, E493D, E494H, and E494T. Although the inhibitor binding screening only showed a significant difference between WT SERT and W103A, no changes occurred for the inhibitor binding affinities with W103A (Figure 5). SSRI serotonin uptake inhibition potency increased as much as 6-fold with the TM1 W103A mutation. The screening for inhibitor binding and substrate uptake at hSERT showed that the created mutants were functional and bound inhibitors and transported substrate. This functionality was at a higher rate than the non-transfected naïve N2A cells (Figure 5). The results of the functionality of the transporter, as measured by the substrate uptake assay, correlated with the substrate uptake assay screening for most of the mutants. Further information on the residue in question can be gained by identifying which amino acids restore function at that position.

Net specific [^{3}H]-serotonin uptake at W103A fell approximately 2-fold even though B_{max} value for [^{125}I]-RTI-55 saturation binding was not significantly affected (0.8 vs. 0.8nM). This suggests that, although binding is not altered with the alanine substitution, the ability of the transporter to transport substrate into the cell has been decreased. LeuT-TCA cocrystals show a salt bridge formed by the transmembrane where W103 is located and TM10 (Sinning et al., 2009). Specifically, this salt bridge is between Arg104 and Glu493, so the W103A mutant could be causing a rotation of TM1, thus disrupting the ability of the transporter to uptake substrate, making this result expected.

Cocaine binding affinity decreased by 2-fold at the V489F mutant. This result suggests that V489 plays a role in cocaine binding, either by directly altering the binding of cocaine or by indirectly destabilizing the binding pocket. Surprisingly, affinity for the cocaine analog RTI-55 increased 2-fold at the V489F mutant as well as at the K490T mutant. This result suggests that the TM10 V489 residue may be in the vicinity of the C-3 tropane substituent of each drug. Interestingly, the V489F substitution increased potency 2-fold to citalopram, but not to sertraline. Binding affinities to citalopram, sertraline, and cocaine were unaffected with the K490T mutation, as well as the uptake capacities. The differences seen between the binding and uptake profiles of the V489F mutant and the K490T mutant may suggest differing roles within the binding pocket of hSERT.

An amino acid of SERT which is consistently suggested to have a role in binding via docking of known inhibitors is the negatively charged and hydrophilic E493. This

glutamic acid is thought to be a part of an extracellular charged gate between TM1 and TM10. Inhibitor binding can induce a formation of this salt bridge in SERT, thus substrate will be unable to translocate across the cell membrane. Similar salt bridges are predicted in other MATs, thus making E493 a logical place to mutate and subsequently expect decreased inhibitor binding. In our study, the conservative E493D mutation decreased binding affinity to citalopram, sertraline, and cocaine. It also decreased uptake inhibition of citalopram and sertraline by 3- and 7-fold, respectively. Although SSRI serotonin uptake inhibition potency increased as much as 6-fold with the TM1 W103A mutation, potency decreased 6-fold at the TM10 E493D mutant. As discussed earlier, this could be due to the role played by the salt bridge between these transmembrane.

At the next amino acid in the hSERT sequence, two mutants were created and tested for inhibitor binding and substrate uptake. E494H and E494T mutations decreased binding affinity to citalopram by 3- and 2-fold, respectively, and E494H decreased uptake inhibition of citalopram by 3-fold, but did not change uptake inhibition of at the E494T substitution. The lack of effect of the E494T substitution on the uptake inhibition of citalopram can be explained based on the charge-neutrality of threonine. Citalopram potency decreased 3-fold at E494H but not at the charge-neutral E494T substitution. The conservative change was not expected to create a large change in binding affinities or in the folding of the protein.

Citalopram binding affinity decreased 3-fold at E493D and E494H SERT, and by over 2-fold at E494T SERT. Interestingly, sertraline affinity decreased 7-fold with the

conservative E493 substitution but was unaffected by the E494 mutations. Because the E493 and E494 side chains are expected to diverge in space, loss of one glutamate side chain should not be compensated for by the presence of the other. Net specific [^{3}H]-serotonin uptake at both E494 SERT mutants fell approximately 2-fold even though B_{max} values for [^{125}I]-RTI-55 saturation binding were not significantly affected. This result implies the glutamic acid at 493 was unable to compensate for either of the mutations at 494. As stated previously, this phenomenon of Net specific [^{3}H]-serotonin uptake decreasing although B_{max} values for [^{125}I]-RTI-55 saturation binding were not significantly affected also occurred with the W103A mutant.

The pharmacological data suggest that when mutated singly, no one of the five SERT vestibular pocket residues surveyed is critical for high affinity binding of cocaine or the two SSRIs tested. These results are consistent with similar vestibular pocket SERT mutants (Anderson, 2009). If a mutant shows impaired SERT inhibitor binding, it would be consistent with the idea that the endogenous amino acid(s) plays a role in the binding process and would be partial confirmation that the binding pocket was identified.

Due to the many unwanted side-effects generated by current antidepressants, such as sleep disruption, weight gain, nausea, as well as slow onset of action (Moret et al., 2009), new therapeutics are sought for development. Drug development is an expensive and time-consuming endeavor. Recently, in silico models have not only been used to guide mutagenesis studies, but also to virtually screen compounds in order to identify potential new structural scaffolds. Virtual screening is an innovative approach to find choice molecules from a large collection of molecules which fit certain criteria, such as potential ability to bind to a specific protein or novel chemical structure. Our study aimed to identify compounds with new structural scaffolds that bind to SERT using computational models of SERT.

The first hSERT model to be used for virtual screening was created by Martin Indarte. This model, referred to as the MI model, used two online alignment servers. Molecular dynamics, which is a xxx used for complex systems in order to determine macroscopic thermodynamic properties of the system, were not performed on this model for the purpose of refinement.

Compounds found to be hits using the MI SERT model were ranked based on the scoring function as described in the methods. Fourteen of the top hit compounds from the MI SERT model were acquired based on price and availability for pharmacological testing and labeled as the LM series. One-point binding assays were performed using HEK cells expressing hSERT with the LM compounds. [^{125}I]-RTI-55 was used as the radioactive competitor in the binding experiments. One-point binding assays using clomipramine

was performed as positive control and buffer as negative control and total [^{125}I]-RTI-55 binding.

As seen collectively in Figure 6, none of the 14 compounds screened as "hits" from the MI SERT model inhibited [^{125}I]-RTI-55 binding at SERT more than the arbitrarily-set threshold of 50%. This threshold was set as a standard guidepost based on the high concentration of drug (10μM) used to compete with [^{125}I]-RTI-55 binding. When homology models are used without refinement, and without X-ray structures of the targets, only low micromolar (1-10uM) activities can be visualized (Zuccotto et al., 2001). Also, the number of compounds that are found as hits is typically very low (Schneider and Bohm, 2002), so these results can be viewed as a reason to revise and refine the SERT model.

The second hSERT model to be used for virtual screening was created by Sankar Manepalli. This model, referred to as the SM model, used alternative methods to the MI model. Four different alignments (Yamashita, Beuming, JACS, etc) were used to create preliminary SERT models. Using additional alignment can improve the precision of the model, as the eventual model was chosen based on a final alignment which was created. The SM model was also refined in two different ways. Ramachandran plots, which are used as a way to visualize backbone dihedral angles of amino acid residues in protein structures, was used in with the *in silico* SERT model and highlighted outliers from the model. The highlighted outliers were minimized to determine their reason for being outliers. Loops, which are a part of the protein that interact with the surrounding aqueous

environment, tend to have charged and polar amino acids and are frequently a component of active sites. Refinement of these loops was also done via visual inspection of the model. Other important differences that could lead to differences in screening outcomes include the orientation of the E493 and E494 functional groups. The MI model shows these functional groups to be both facing toward the inhibitor binding pocket, while the SM pocket determined the E494 functional group to be facing away from the pocket. The SM model orientation of these two amino acids is seen as a confirmation as to why the neighboring glutamic acids do not compensate for the other upon mutation of one.

Using the SM model, two sets of compounds were chosen for pharmacological testing. The first set acquired and tested were 10 compounds which were of higher ranking and labeled as the SM series. The second set were 11 compounds which were of lower ranking and labeled as the MS series. One-point binding assays were performed using HEK cells expressing hSERT, hDAT, or hNET with the hit compounds from the SM series from the MI SERT model. The compounds were tested in not only cells expressing hSERT, but also cells expressing hDAT and cells expressing hNET due to the similarity among the monoamine transporters.

At the cells expressing hNET, the SM series compounds did not significantly inhibit [^{125}I]-RTI-55 binding in a one-point binding assay. Although there is a large amount of sequence similarity between the monoamine transporters, differences may exist between the inhibitor binding pockets which may make some compounds more selective for a

specific transporter over the others. In this case, the compounds screened as hits using a hSERT model did not inhibit hNET.

At the cells expressing hDAT, one compound from the SM series inhibited [^{125}I]-RTI-55 binding in a one-point binding assay. Although SM14 displayed no significant binding to hSERT, it appeared to inhibit [^{125}I]-RTI-55 binding to hDAT by 40%. A binding assay was completed and found that this compound had a low uM affinity to hDAT and inhibited substrate translocation at similar concentrations. The amount of sequence similarity between the dopamine transporter and the serotonin transporter makes it more likely for a compound screened to dock at the SERT pocket to also dock at the DAT pocket.

At the cells expressing hSERT, two compounds from the SM series inhibited [^{125}I]-RTI-55 binding in a one-point binding assay. Labeled as SM10 and SM11, these compounds were not only found to bind to hSERT with appreciable affinity, but were also found to have a selective affinity for SERT over the dopamine transporter and norepinephrine transporter. These results are encouraging, as the compounds emerged from a virtual screening experiment utilizing a large database and a comparative SERT protein model with low sequence similarity to its template.

The second set were 11 compounds which were of lower ranking than the SM series, and were labeled as the MS series. One-point binding assays were performed using HEK cells expressing hSERT, hDAT, or hNET with the hit compounds from the MS series

from the MI SERT model. Just like the previous compounds found via virtual screening of these SERT models, the compounds were tested in not only cells expressing hSERT, but also cells expressing hDAT and cells expressing hNET due to the similarity among the monoamine transporters. Unfortunately, none of this second set of lower ranking hit compounds were found to inhibited [^{125}I]-RTI-55 binding at SERT more than the arbitrarily-set threshold of 50%.

The differences in the number of compounds that emerge as hit compounds can be a consequence of the differences in sequence alignments and models. Models are not perfect, but can be useful. This model evolved due to new information from pharmacological testing and mutagenesis, which lead to the discovery of two novel scaffolds which are capable of inhibiting a cocaine analog from binding to the transporter.

Future directions for this research will aim to further define the SERT inhibitor binding pockets. One promising avenue of research would be to localize SSRI-based photoprobes to the SERT S1 or S2 binding pocket. This would be done using the analogs created with clickable handles and pharmacologically tested at SERT. A SERT-ligand irreversible covalent could be induced by exposing the protein-ligand complex to ultraviolet light (Lapinsky, 2012). Subsequently, liquid chromatography-mass spectrometry (LC/MS) would be used for its high sensitivity and selectivity to identify specific acids which form bonds with the probe. Another promising avenue of research would be the behavioral testing of the VS compounds found to bind with high affinity to

the SERT in an *in vivo* model of depression or anxiety. Positive results would highlight the importance and advantages of using an *in silico* model for the discovery of novel therapeutics.

REFERENCES

Alonso, R., Griebel, G., Pavone, G., Stemmelin, J., Le Fur, G., Soubrie, P. (2004). Blockade of CRF(1) or V(1b) receptors reverses stress-induced suppression of neurogenesis in a mouse model of depression. *Mol Psychiatry, 9;* 278-286

Anand, K., Ziebuhr, J., Wadhwani, P., Mesters, J.R., and Hilgenfeld, R. (2003). Coronavirus main proteinase (3CLpro) structure: basis for design of anti-SARS drugs. *Science, 300;* 1763-1767

Andersen, J., Taboureau, O., Hansen, K., Olsen, L., Egebjerg, J., Stromgaard, K., and Kristensen, A. (2009). Location of the Antidepressant Binding Site in the Serotonin Transporter. *J. Biological Chem. 284(15);* 10276-10284

Bailey, D., and Brown, D. (2001). High-throughput chemistry and structure-based design: survival of the smartest. *Drug Discov Today, 6;* 57-59

Barker, E., Perlman, M., Adkins, E., Houlihan, W., Pristupa, Z., Niznik, H., Blakely, R. (1998). High Affinity Recognition of Serotonin Transporter Antagonists Defined by Species-scanning Mutagenesis. *J. Biological Chem. 273.* 19459-19468

Beuming, T., Shi, L., Javitch, J.A., and Weinstein, H. (2006). A comprehensive structure-based alignment of prokaryotic and eukaryotic neurotransmitter/Na+ symporters (NSS)

aids in the use of the LeuT structure to probe NSS structure and function. *Mol. Pharmacol. 70.* 1630-1642.

Beuming, T., Kniazeff, J., Bergmann, M., Shi, L., Gracia, L., Raniszewska, K., Newman, A., Javich, J., Weinstein, H., Gether, U., and Loland, C. (2008). The binding sites for cocaine and dopamine in the dopamine transporter overlap. *Nature Neuroscience. 11(7). 780-789.*

Bourin, M., Chenu, F., Ripoll, N., David, D.J.P. (2005). A proposal of decision tree to screen putative antidepressants using forced swim and tail suspension tests. *Behavioral Brain Research. 164;* 266-269

Brunton L L, Blumenthal D K, Murri N, Dandan R H, Knollmann B C. (2011). *Goodman & Gilman's The Pharmacological Basis of Therapeutics*. 12th ed. New York: McGraw-Hill

Carlson, H.A. and McCammon, J.A. (2000). Accommodating protein flexibility in computational drug design. *Mol Pharmacol, 57;* 213-218

Cryan, J.F., Mombereau, C., Vassout, A. (2005). The tail suspension test as a model for assessing antidepressant activity: review of pharmacological and genetic studies in mice. *Neurosci Biobehav Rev. 29(4-5);* 571-625

Davis, A.M., Teague, S.J., and Kleywegt, G.J. (2003). Application and limitations of X-ray crystallographic data in structure-based ligand and drug design. *Angew Chem Int Ed Engl, 42;* 2718-2736

Dunbrack, RL., Jr. (2006). Sequence comparison and protein structure prediction. *Curr Opin Struct Biol. 16;* 374-384

Dulawa, S.C., Hen, R. (2005). Recent advances in animal models of chronic antidepressant effects: the novelty-induced hypophagia test. *Neurosci Biobehav Rev. 29(4-5);* 771-783

Eison, A.S., and Mullin, U.L. (1996). Regulation of central 5-HT2A receptors: a review of in vivo studies. *Behavioral Brain Research. 73(1-2);* 177-181

Evers, A., Hessler, G., Matter, H., and Klabunde, T. (2005). Virtual screening of biogenic amine-binding G-Protein coupled receptors: comparative evaluation of protein- and ligand-based virtual screening protocols. *J Med Chem, 48;* 5448-5465

Forrest, L, Tavoulari, S., Zhang, Y., Rudnick, G., Honig, B. (2007). Identification of a chloride ion binding site in Na^+/Cl^--dependent transporters. *Proc. Natl. Acad. Sci. U.S.A. 104;* 12761-12766

Goldberg, N.R., Beuming, T., Soyer, O.S., Goldstein, R.A., Weinstein, H, and Javitch, J.A. (2003). Probing conformational changes in neurotransmitter transporters: a structural context. *Eur J Pharmacol, 479;* 3-12

Gubbens, J., Ruijter, E., de Fays, L.E., Damen, J.M., de Kruijff,B., Slijper, M., Rijkers, D.T., Liskamp, R.M., de Kroon, A.I. (2009). Photocrosslinking and click chemistry enable the specific detection of proteins interacting with phospholipids at the membrane interface. *Chem Biol, 16*: 3-14

Henry, L.K., Adkins, E.M., Han, Q., and Blakely, R.D. (2003). Serotonin and cocaine-sensitive inactivation of human serotonin transporters by methanethiosulfonates targeted to transmembrane domain I. *J Biol Chem, 278;* 37052-37063

Henry, L.K., Field, J.R., Adkins, E.M., Parnas, M.L., Vaughan, R.A., Zou, M.F., Newman, A.H., and Blakely, R.D. (2006). Tyr-95 and Ile-172 in transmembrane segments 1 and 3 of human serotonin transporters interact to establish high affinity recognition of antidepressants. *J Biol Chem, 281;* 2012-2023

Henry, L.K., Iwamoto, H., Field, J.R., Kaufmann, K., Dawson, E.S., Jacobs, M.T., Adams, C., Felts, B., Zdravkovic, I., Armstrong, V., Combs S., Solis, E., Rudnick, G., Noskov, S.Y., Defelice, L.J., Meiler, J., R.D. Blakely, R.D. A Conserved Asparagine Residue in Transmembrane Segment 1 (TM1) of Serotonin Transporter Dictates Chloride-coupled Neurotransmitter Transport. *J Biol Chem. 286*: 30823-36.

Hillisch, A., Pineda, L.F., and Hilgenfeld, R. (2004). Utility of homology models in the drug discovery process. *Drug Discov Today. 9;* 659-669.

Hirani, K., Khisti, R. T., Chopde, C.T. (2002) Behavioral action of ethanol in Porsolt's forced swim test: modulation by 3 alpha-hydroxy-5 alpha-pregnan-20-one. *Neuropharmacology* 43(8):1339-50.

Holick, K.A., Lee, D.C., Hen, R., Dulawa, S.C. (2008). Behavioral effects of chronic fluoxetine in BALB/cJ mice do not require adult hippocampal neurogenesis or the serotonin 1A receptor. *Neuropsychopharmacology, 33;* 406-417

Holmes, A., Yang., Murphy, D., Crawley, J.N. (2002). Evaluation of antidepressant-related behavioral responses in mice lacking the serotonin transporter. *Neuropsychopharmacology,27 (6);* 914-923

Hristozov, D.P., Oprea, T.I., and Gasteiger, J. (2007). Virtual screening applications: a study of ligand-based methods and different structure representations in four different scenarios. *J Comput Aided Mol Des, 21;* 617-640

Indarte, M., Madura, J.D., Surratt, C.K. (2008). Dopamine transporter comparative molecular modeling and binding site prediction using the LeuT (Aa) leucine transporter as a template. *Proteins, 70;* 1033-1046

Kaufmann, K, Dawson, E., Henry, K., Field, J., Blakely, R., Meiler, J. (2009). Structural determinants of species-selective substrate recognition in human and *drosophila* serotonin transporters revealed through computational docking studies. *Proteins. 74;* 630-642

Lapinsky, D. (2012). Tandem photoaffinity labeling-bioorthogonal conjugation in medicinal chemisty. *Bioorganic and Medicinal Chemistry, 20;* 6237-6247

Loland, C.J., Granas, C., Javich, J.A., and Gether, U. (2004). Identification of intracellular residues in the dopamine transporter critical for regulation of transporter conformation and cocaine binding. *J Biol Chem, 279;* 3228-3238

MacMillan, K.S., Naidoo, J., Liang, J., Melito, L, Williams, N., Morlock, L.,Huntington, P.J., Estill, S.J., Longgood, J., Becker, G.L., McKnight, S.L., Pieper, A.A., De Brabander, J.K., Ready, J.M. (2011). Development of proneurogenic, neuroprotective small molecules. *JACS, 133;* 1428-1437

Malberg, J.E., Eisch, A.J., Nestler, E.J., Duman, R.S. (2000). Chronic antidepressant treatment increases neurogenesis in adult rat hippocampus. *J. Neurosci., 20 (4);* 9104-9110

Manepalli, S., Geffert, L.M., Surratt, C.K., Madura, J.D. (2011). Discovery of novel selective serotonin reuptake inhibitors through development of a protein-based pharmacophore. *J Chem Information and Modeling. 51;* 2417-2426

Matthew, E.E., Zoonens, M., and Engelman, D.M. (2006). Dynamic helix interactions in transmembrane signaling. *Cell. 127;* 447-450

Moret, C., Isaac, M., Briley, M (2009). Problems associated with long-term treatment with selective serotonin reuptake inhibitors. *J Psychopharmacol, 23*: 967-74.

Moustakas, D.T., Lang, P.T., Pegg, S., Pettersen, E., Kuntz, I.D., Brooijmans, N., and Rizzo, R.C. (2006). Development and validation of a modular, extensible docking program: DOCK5. *J Comput Aided Mol Des, 20;* 601-619

Nolan, T.L., Lapinsky, D.J., Talbot, J.N., Indarte, M., Liu, Y., Manepalli, S., Geffert, L.M., Amos, M.E., Taylor, P.N., Madura, J.D., Surratt, C.K. (2011). Identification of a novel selective serotonin reuptake inhibitor by coupling monoamine transporter-based virtual screening and rational molecular hybridization. *ACS Chem Neuro. 2(9);* 544-552

Petrey, D., and Honig, B. (2005). Protein structure prediction: inroads to biology. *Mol Cell. 20;* 811-819

Pieper, U., Eswar, N., Stuart, A.C., Ilyin, V.A., and Sali, A. (2002). MODBASE, a database of annotated comparative protein structure models. *Nucleic Acids Res. 30;* 255-259

Schneider, G. and Bohm, H.J. (2002). Virtual screening and fast automated docking methods. *Drug Discov Today, 7;* 64-70

Sinning, S., Musgaard, M., Jensen, M., Severinsen, K., Celik, L., Koldso, H., Meyer, T., Bols, M., Jensen, H., Schiott, B., Wiborg, O. (2009). Binding and orientation of tricyclic antidepressants within the central substrate site of the human serotonin transporter. *Journal of Biological Chemistry. 10;* 1074-1087

Surratt, C.K. and Adams, W.R. (2005). G protein-coupled receptor structural motifs: relevance to the opioid receptors. *Curr Top Med Chem, 5;* 315-324

Surratt, C.K., Ukairo, O.T., and Ramanujapuram, S. (2005). Recognition of psychostimulants, antidepressants, and other inhibitors of synaptic neurotransmitter uptake by the plasma membrane monoamine transporters. *AAPS J, 7;* 739-751

Takayama, H. and Sugio, S. (2011). Functional expression of milligram quantities of the synthetic human serotonin transporter gene in a tetracycline-inducible HEK293 cell line. *Protein Expr Purif. 76*: 211-20

Talbot, J. N., Jutkiewicz, E. M., Graves, S. M., Clemans, C. F., Nicol, M. R., Huang, X., Mortensen, R. M., Neubig, R. R., and Traynor, J. R. (2010) RGS inhibition selectively potentiates serotonin-mediated antidepressant effects. Proc. Natl. Acad. Sci. U.S.A. 107, 11086–11091.

Vaughan, R.A., M.L. Parnas, ML., Gaffaney, J.D., Lowe, M.J., Wirtz, S., Pham, A., Reed, B., Dutta, S.M., Murray, K.K., Justice, J.B. (2005). Affinity labeling the dopamine transporter ligand binding site. *J Neurosci Methods, 143*: 33-40

Weerapana, E., Speer, A.E., Cravett, B.F. (2007). Tandem orthogonal proteolysis-activity-based protein profiling (TOP-ABPP)--a general method for mapping sites of probe modification in proteomes. *Nat Protoc, 2*: 1414-25

Yamashita, A., Singh, S.K., Kawate, T., Jin, Y., and Gouaux, E. (2005). Crystal structure of a bacterial homologue of Na+/Cl- -dependent neurotransmitter transporters. *Nature. 437,* 215-223

Zhou, Z., Zhen, J., Karpowich, N., Law, C., Reith, M., and Wang, D. (2009). Antidepressant specificity of serotonin tranporter suggested by three LeuT-SSRI structures. *Nature Structural & Molecular Biology. 16(6);* 652-658